Event-Triggered Formation Control and Leader Tracking With Resilience to Byzantine Adversaries: A Reputation-Based Approach

Federico M. Zegers, Matthew T. Hale, *Member, IEEE*, John M. Shea, *Member, IEEE*, and Warren E. Dixon, *Fellow, IEEE*

***Abstract*—A distributed event-triggered controller is developed for formation control and leader tracking (FCLT) with robustness to adversarial Byzantine agents for a class of heterogeneous multi-agent systems (MASs). Assuming each agent can accurately measure the state of a neighbor whenever the neighbor broadcasts its state, a reputation-based strategy is developed for each agent to detect Byzantine agent behaviors within their neighbor set and then selectively disregard Byzantine state information. Selectively ignoring Byzantine agents results in a time-varying graph topology. Nonsmooth dynamics also result from intermittent communication due to an event-triggered strategy, which facilitates the efficient use of resources. Nonsmooth Lyapunov methods are used to prove stability and FCLT of the MAS consisting of the remaining cooperative agents.**

***Index Terms*—Decentralized control, fault tolerant control, multi-agent systems, networked control systems.**

I. Introduction

EVENT-TRIGGERED control (ETC) is an intermittent state feedback strategy motivated by advantages such as the efficient use of resources, like communication energy and bandwidth, through trigger-based sensing, actuation, and/or communication (see [1]–[5]) and the ability to design the trigger condition to ensure stability properties [6]. ETC has been applied for the coordination of multi-agent systems (MASs), especially in mobile network applications, given the limited energy in portable power supplies and constrained networks available in operational scenarios (see [2], [3], [7]). Results such as [1], [3], [5], [8], and [9], among many others, are developed under the implicit assumption that the MASs operate in a benign environment that is free from adversaries (i.e., all agents are cooperative in the sense that they communicate true state information and follow the network objective).

With respect to ETC, if the update of state variables is delayed and/or updated with incorrect information, the resulting system performance may degrade, especially if state updates are infrequent. Because the communication timing conditions of ETC methods create potential vulnerabilities, resilient strategies are motivated for assured coordination in contested environments. Common threats in contested environments include: Denial-of-service (DoS) attacks, time-delay switch (TDS) attacks, and Byzantine attacks. A DoS attack occurs when an adversary interrupts communication within a network [10]; a TDS attack occurs when an adversary imparts time delays on communication within a network [11]; and a Byzantine attack is a more general threat where communication can be delayed, corrupted, and/or interrupted arbitrarily [12].

In this article, we focus on Byzantine threats since they are a generalization of DoS and TDS attacks. As in [13], we consider two types of Byzantine behavior. A Type I Byzantine agent remains in the mobile network, where it can halt, delay, or corrupt information communicated to its neighbors temporarily or indefinitely. A Type II Byzantine agent abandons the mobile network while communicating true or no state information about itself temporarily or indefinitely. These designations are not fixed for all time, and any adversary can be categorized as either type at any time.

Results, such as [14]–[16], attain consensus in the presence of Type I Byzantine adversaries. However, they are not able to identify Byzantine threats nor can they alter the communication network to stop data sharing between the cooperative and Byzantine agents as in [13]. In [13], Byzantine adversaries are identified through a Lyapunov-based detector that compares communicated state information to worst-case state estimates that are based on accurate past neighbor state information. While such a strategy enables Byzantine agent detection, it is limited in the sense that the detector requires an upper bound on the control of each neighboring agent, which may be unknown *a*

Manuscript received September 7, 2020; revised September 15, 2020 and January 22, 2021; accepted February 21, 2021. Date of publication March 23, 2021; date of current version September 17, 2021. This work was supported in part by a Task Order contract with the Air Force Research Laboratory, Munitions Directorate at Eglin AFB, Office of Naval Research under Grant N00014-13-1-0151, in part by NEEC Grant N00174-18-1-0003, and in part by AFOSR Grant FA9550-18-1-0109 and Grant FA9550-19-1-0169. Recommended by Associate Editor I. Lestas. *(Corresponding author: Federico Zegers.)*

Federico M. Zegers and Matthew T. Hale are with the Department of Mechanical and Aerospace Engineering, University of Florida, Gainesville, FL 32611-6250 USA (e-mail: fredzeg@ufl.edu; matthewhale@ufl.edu).

John M. Shea is with the Department of Electrical and Computer Engineering, University of Florida, Gainesville, FL 32611-6250 USA (e-mail: jshea@ece.ufl.edu).

Warren E. Dixon is with the Department of Mechanical and Aerospace Engineering and also with the Department of Electrical and Computer Engineering, University of Florida, Gainesville, FL 32611-6250 USA (e-mail: wdixon@ufl.edu).

Digital Object Identifier 10.1109/TCNS.2021.3068348

priori. Moreover, once an agent is categorized as a Byzantine adversary, it cannot be reincorporated back into the cooperative neighbor set even if it becomes cooperative. Such a scenario can occur when the communication links between a group of cooperative agents are temporarily jammed by an adversary. These limitations can potentially be circumvented through the use of a reputation algorithm [17], which does not require exact model knowledge of each neighbor's dynamics, does not require bounds on neighbor quantities such as control, and enables the reintegration of rehabilitated agents, i.e., agents that convert from Byzantine to cooperative.

In this work, we expand our precursory result in [13] and investigate formation control and leader tracking (FCLT), also referred to as leader–follower formation control in [18], in the presence of Byzantine adversaries. Specifically, FCLT refers to a set of follower agents tracking the trajectory of a leader agent while the follower agents preserve a predefined formation. The Byzantine adversaries are assumed to operate independently, i.e., Byzantine agents do not work together against the cooperative followers. Since only the cooperative followers must collaborate to perform secure FCLT, a traditional unsigned graph is used to model the network of cooperative followers. Moreover, an ETC method is developed that facilitates assured FCLT while promoting the efficient use of resources and providing resilience to Byzantine adversaries. While the coordination strategy in [13] relies on exact model knowledge, this result enables coordination for agents modeled with uncertain nonlinear dynamics subject to an exogenous disturbance.

Inspired by the reputation-based method for adjusting the network edge weights in [17], we develop a reputation-based Byzantine detection strategy that enables coordination between cooperative agents only, while enabling the capability of reintegrating rehabilitated agents. The reputation strategy also enables malfunctioning agents to be isolated from the cooperative MAS to ensure safety and enable the remaining agents to achieve the objective. A malfunctioning agent can be reintegrated into the network once functional operational control can be established. By coordinating only with cooperative neighbor information, the influence from each Byzantine adversary is cut out from the network consisting of only the cooperative followers. The Byzantine detection strategy is based on two-point authentication, e.g., comparing communicated and sensed state information, where the redundancy in state information enables Byzantine agent detection. Stability of the ETC strategy is examined through nonsmooth Lyapunov analysis.

In our preliminary result in [19], we established the concept of using a zero-order hold to enable formation control and leader tracking with intermittent communication between the followers only and the use of trust and reputation models to impart resilience to Byzantine adversaries. In this article, a more complete development of the ideas in [19] is provided by: 1) A revised, more detailed, and more rigorous narrative and presentation; 2) a generalization of the mathematics to relax the previous requirement of continuous communication with the leader to allow only intermittent feedback; 3) a proof of the existence of a positive uniform lower bound for the difference between consecutive broadcast events for each agent, including the leader; and 4) simulation results that demonstrate the performance of the developed methods.

II. Preliminaries

A. Notation

Let $\mathbb{R}$ and $\mathbb{Z}$ denote the sets of real numbers and integers, respectively, where $\mathbb{R}_{\geq 0} \triangleq [0, \infty)$,$\mathbb{R}_{>0} \triangleq (0, \infty)$, $\mathbb{Z}_{\geq 0} \triangleq \mathbb{R}_{\geq 0} \cap \mathbb{Z}$, and $\mathbb{Z}_{>0} \triangleq \mathbb{R}_{>0} \cap \mathbb{Z}$. Let $p, q, n \in \mathbb{Z}_{>0}$. The $p \times q$ zero matrix and the $p \times 1$ zero column vector are denoted by $0_{p\times q}$ and 0_p, respectively. The $p \times p$ identity matrix and the $p \times 1$ ones column vector are denoted by I_p and 1_p, respectively. The Euclidean norm of a vector $r \in \mathbb{R}^p$ is denoted by $\|r\| \triangleq \sqrt{r^\top r}$. The Frobenius norm of $A \in \mathbb{R}^{p\times q}$ is denoted by $\|A\|_F \triangleq \sqrt{1_p^\top (A \odot A) 1_q}$, where $\odot$ denotes the Hadamard product. The block diagonal matrix, whose diagonal blocks consist of $G_1, G_2, \ldots, G_n \in \mathbb{R}^{p\times q}$, is denoted by $\operatorname{diag}(G_1, G_2, \ldots, G_n) \in \mathbb{R}^{np\times nq}$. Given a symmetric matrix $A \in \mathbb{R}^{n\times n}$, $\lambda_{\min}(A), \lambda_{\max}(A)$, and $\lambda_i(A)$ denote the minimum, maximum, and ith eigenvalue of A, respectively. The class C^1 refers to the set of continuously differentiable functions. Let f be an essentially bounded measurable function. Then, $f \in \mathcal{L}_\infty$ if and only if $\inf\{C \geq 0 : |f(x)| \leq C$ for almost every $x\} \in \mathbb{R}_{\geq 0}$. The Kronecker product of $A \in \mathbb{R}^{p\times q}$ and $B \in \mathbb{R}^{u\times v}$ is denoted by $(A \otimes B) \in \mathbb{R}^{pu\times qv}$. The complement and power set of the set $\mathcal{S}$ are denoted by $\mathcal{S}^C$ and $2^{\mathcal{S}}$, respectively.

B. Algebraic Graph Properties

Let $\mathcal{G}(t) \triangleq (\mathcal{V}, \mathcal{E}(t), \mathcal{A}(t))$ be a time-varying, weighted, and undirected graph with node set $\mathcal{V} \triangleq \{1, 2, \ldots, N\}$, for $N \in \mathbb{Z}_{>0}$, edge mapping $\mathcal{E} : [0, \infty) \to 2^{\mathcal{V}\times\mathcal{V}}$, and weighted adjacency mapping $\mathcal{A} : [0, \infty) \to \mathbb{R}^{N\times N}$, where $\mathcal{A}(t) \triangleq [a_{ij}(t)]$, such that $a_{ij} : [0, \infty) \to [0, 1]$. Within the context of this work, no self-loops are considered and, therefore, $a_{ii}(t) \triangleq 0$ for all $i \in \mathcal{V}$ and for all $t \geq 0$. An undirected edge is defined as an ordered pair (j, i), where $(j, i) \in \mathcal{E}(t)$ if and only if $(i, j) \in \mathcal{E}(t)$. Note that $(j, i) \in \mathcal{E}(t)$ implies agent i can obtain information from agent j and vice versa. An undirected path is a sequence of undirected edges in $\mathcal{E}(t)$. An undirected graph is called connected if and only if there exists an undirected path between any two distinct nodes. The time-varying neighbor set of node i is defined by $\mathcal{N}_i : [0, \infty) \to 2^{\mathcal{V}}$, where $j \in \mathcal{N}_i(t)$ if and only if $(j, i) \in \mathcal{E}(t)$. The weighted degree matrix of the undirected graph $\mathcal{G}(t)$ is defined by $\Delta : [0, \infty) \to \mathbb{R}^{N\times N}$, such that $\Delta(t) \triangleq [\Delta_{ij}(t)]$, where $\Delta_{ij}(t) \triangleq 0$ for all $i \neq j$ and $\Delta_{ii}(t) \triangleq \sum_{j\in\mathcal{V}} a_{ij}(t)$.

The weighted graph Laplacian $L : [0, \infty) \to \mathbb{R}^{N\times N}$ of the undirected graph $\mathcal{G}(t)$ is defined by $L(t) \triangleq \Delta(t) - \mathcal{A}(t)$. Let node 0, where $0 \notin \mathcal{V}$, be independent of the graph structure and $b_{\max} \in \mathbb{R}_{>0}$. Let the diagonal (pinning) matrix encoding the edge weights between node 0 and node $i \in \mathcal{V}$ be defined by $B : [0, \infty) \to \mathbb{R}^{N\times N}$, where $B(t) \triangleq [b_{ij}(t)]$, such that $b_i \triangleq b_{ii} : [0, \infty) \to [0, b_{\max}]$ for all $i \in \mathcal{V}$ and $b_{ij}(t) \triangleq 0$ for all $i \neq j$. If $b_i(t) > 0$, then node i can receive information from node 0. The time-varying weighted connectivity matrix $H : [0, \infty) \to$

$\mathbb{R}^{N\times N}$, encoding the flow of information between all nodes in $\mathcal{V}\cup\{0\}$, is defined by $H(t)\triangleq L(t)+B(t)$.

III. Agent Dynamics and Network Topology

Consider a heterogeneous MAS consisting of a single leader agent indexed by 0 and a set of $N\in\mathbb{Z}_{>0}$ follower agents indexed by $\mathcal{V}$. The uncertain nonlinear model for agent $i\in\mathcal{V}\cup\{0\}$ is

$$\dot{x}_i(t)\triangleq f_i\left(x_i(t)\right)+g_i\left(x_i(t)\right)u_i(t)+d_i(t) \tag{1}$$

where $x_i:[0,\infty)\to\mathbb{R}^n$ denotes the position, $\dot{x}_i:[0,\infty)\to\mathbb{R}^n$ denotes the velocity, $f_i:\mathbb{R}^n\to\mathbb{R}^n$ denotes the uncertain drift dynamics, $g_i:\mathbb{R}^n\to\mathbb{R}^{n\times m}$ denotes the known control effectiveness matrix, $u_i:[0,\infty)\to\mathbb{R}^m$ denotes the control input, and $d_i:[0,\infty)\to\mathbb{R}^n$ denotes an exogenous disturbance for agent i. Let $\mathcal{B}:[0,\infty)\to 2^{\mathcal{V}}$ define the time-varying set of Byzantine agents and $\mathcal{C}:[0,\infty)\to 2^{\mathcal{V}}$ define the time-varying set of cooperative agents, where $\mathcal{B}(t)\cap\mathcal{C}(t)=\varnothing$ and $\mathcal{B}(t)\cup\mathcal{C}(t)=\mathcal{V}$ for all $t\geq 0$. The following assumptions are made to facilitate the subsequent analysis.

Assumption 1: For each $i\in\mathcal{V}\cup\{0\}$, the uncertain drift dynamics f_i is class C^1 and bounded given a bounded argument, i.e., if $\|x(t)\|\leq\bar{c}_1$ for some $\bar{c}_1\in\mathbb{R}_{>0}$, then $\|f_i(x(t))\|\leq\bar{c}_2$ for some $\bar{c}_2\in\mathbb{R}_{>0}$.

Assumption 2: The control effectiveness matrix g_i is C^1, bounded given a bounded argument, and full-row rank for all $i\in\mathcal{V}\cup\{0\}$. Moreover, the right pseudoinverse of g_i is denoted by $g_i^{+}:\mathbb{R}^n\to\mathbb{R}^{m\times n}$, where $g_i^{+}(\cdot)\triangleq g_i^{\top}(\cdot)(g_i(\cdot)g_i^{\top}(\cdot))^{-1}$ is bounded given a bounded argument for each $i\in\mathcal{V}\cup\{0\}$.[1]

Assumption 3: The exogenous disturbance d_i is continuous and bounded in the sense that $\|d_i(t)\|\leq d_{i,\max}$ for all $t\geq 0$ and $i\in\mathcal{V}\cup\{0\}$, where $d_{i,\max}\in\mathbb{R}_{>0}$ is a known bounding constant.

Assumption 4: The leader is cooperative for all $t\geq 0$.[2]

Assumption 5: Agent i is capable of measuring its own position $x_i(t)$ for all $t\geq 0$ and all $i\in\mathcal{V}\cup\{0\}$.

Assumption 6: [17] The control and position of the leader are bounded, i.e., there exist $u_{0,\max},x_{0,\max}\in\mathbb{R}_{>0}$, such that $\|u_0(t)\|\leq u_{0,\max}$ and $\|x_0(t)\|\leq x_{0,\max}$ for all $t\geq 0$.

Assumption 7: For each instant $t\geq 0$ that follower $j\in\mathcal{N}_i(t)$ broadcasts its state to follower i, follower i can accurately measure the state of follower j.

Let $x_{ij}:[0,\infty)\to\mathbb{R}_{\geq 0}$ be defined as $x_{ij}(t)\triangleq\|x_i(t)-x_j(t)\|$. Agent i can broadcast information to agent j if and only if $x_{ij}(t)\leq R_{C,i}$, where $R_{C,i}\in\mathbb{R}_{>0}$ denotes the communication radius of agent i. Similarly, agent i can sense agent j if and only if $x_{ij}(t)\leq R_{S,i}$, where $R_{S,i}\in\mathbb{R}_{>0}$ denotes the sensing radius of agent i. Without loss of generality, let $R\triangleq\min\limits_{i\in\mathcal{V}}\{R_{C,i},R_{S,i}\}\in\mathbb{R}_{>0}$, where R is defined as the interaction radius of all agents in the MAS. The neighbor set of follower i is given by $\mathcal{N}_i(t)\triangleq\{j\in\mathcal{V}:x_{ij}(t)\leq R\}$, where followers i and $j\in\mathcal{N}_i(t)$ can both broadcast information to and sense each other. Followers i and j are said to be paired if and only if $i\in\mathcal{N}_j(t)$ and $j\in\mathcal{N}_i(t)$. Similarly, followers i and j are said to be connected if and only if $a_{ij}(t)\neq 0$ and $a_{ji}(t)\neq 0$.

Observe that follower i can be influenced by follower j if and only if $a_{ij}(t)\neq 0$. The influence relationships between the followers of the MAS are modeled by a time-varying, weighted, and undirected graph $\mathcal{G}(t)\triangleq(\mathcal{V},\mathcal{E}(t),\mathcal{A}(t))$. Let $\mathcal{E}_C(t)$ denote the undirected edge set and $\mathcal{A}_C(t)$ denote the weighted adjacency matrix associated with all cooperative followers in $\mathcal{C}(t)$. Moreover, the sub-MAS consisting of only the cooperative followers is modeled by the time-varying, weighted, and undirected graph $\mathcal{G}_C(t)\triangleq(\mathcal{C}(t),\mathcal{E}_C(t),\mathcal{A}_C(t))$ and is referred to as the cooperative MAS (CMAS).

Assumption 8: The graph $\mathcal{G}_C(t)$ is connected for all $t\geq 0$, and $b_i(t)>0$ for some $i\in\mathcal{C}(t)$ for all $t\geq 0$.[3]

Remark 1: Assumptions 4 and 8 ensure that each cooperative agent has at least one cooperative neighbor for all $t\geq 0$, even in the presence of a DoS attack. Moreover, Assumptions 4 and 8 ensure that the Byzantine agents cannot enter the MAS in a manner that partitions $\mathcal{G}_C(t)$ for any $t\geq 0$.

IV. Objectives

The goal is to design distributed controllers for all followers in the MAS that maneuver the followers to a desired formation while tracking the leader. However, as FCLT is taking place, some followers may transform into Byzantine agents as a result of operating within a contested environment, e.g., if they suffer cyber-attacks. The objective is to design distributed controllers for all followers $i\in\mathcal{V}$ governed by (1) that enable the cooperative followers to achieve FCLT while identifying Byzantine agents and removing all Byzantine influence from the CMAS. The distributed controllers are event-triggered to promote the efficient use of communication and sensing resources. Cooperative and Byzantine agents are managed through the edge weight policy, which is based on a reputation algorithm. The policy enables all agents to differentiate between cooperative and Byzantine neighbors, coordinate their motion by using only information from cooperative neighbors, and reintegrate agents into the CMAS once an agent converts from Byzantine to cooperative. The separation between communication and influence is made to enable the reintegration of remediated followers, which requires communication between cooperative–Byzantine pairs. The ability to reintegrate cooperative agents is key for defense against adversarial behaviors such as mobile jammers that can temporarily affect agents before moving on to jam other agents. To quantify the objective, let the FCLT error $e_{1,i}:[0,\infty)\to\mathbb{R}^n$ be defined as

$$e_{1,i}(t)\triangleq x_i(t)-x_0(t)-v_i \tag{2}$$

where $v_i\in\mathbb{R}^n$ denotes the desired relative position between follower i and the leader.

[1]The assumption of a full-row rank control effectiveness matrix is potentially restrictive for some applications (e.g., underactuated systems) and is a topic for future investigation. For LTI systems with a full-column rank control effectiveness matrix, the algebraic Riccati equation or linear matrix inequalities can potentially be used to develop stabilizing controllers.

[2]In the absence of a manned leader, multiple leaders can be added to the MAS through the pinning matrix strategy to impart additional resilience to Byzantine adversaries. Assumption 4 can then be reduced to requiring that at least one leader is cooperative for all time.

[3]An alternative to Assumption 8 is to assume $\mathcal{G}_C(t)$ is connected for all time, upper bound the number of Byzantine adversaries within a network by $f\in\mathbb{Z}_{>0}$, use more than f leaders, and employ connectivity models like the $2f+1$ model described in [14].

Assumption 9: The relative position vector v_i is fixed for all $i \in \mathcal{V}$. Moreover, each follower knows v_i for all $i \in \mathcal{V}$, i.e., each follower knows the entire formation.

By allowing each follower to know v_i for all $i \in \mathcal{V}$, any rehabilitated agent can be reintegrated into any available formation vacancy, if there are multiple options. The FCLT problem can be converted into a leader–follower consensus problem provided $v_i \triangleq 0_n$ for all $i \in \mathcal{V}$. The use of ETC also motivates the development of an estimator to provide continuous state estimates between communication events. The state estimation error of follower i is defined by $e_{2,i} : [0,\infty) \to \mathbb{R}^n$, where

$$e_{2,i}(t) \triangleq \hat{x}_i(t) - x_i(t) \tag{3}$$

such that $\hat{x}_i : [0,\infty) \to \mathbb{R}^n$ denotes the state estimate of x_i.

V. Controller Development

A. Trust Model

As Byzantine agents emerge in the MAS, the remaining cooperative followers require a method to identify their cooperative neighbors. Let $\tau_{ij} : [0,\infty) \to [0,1]$ denote the piecewise constant trust that follower i has in follower $j \in \mathcal{N}_i(t)$, where 0 and 1 represent no trust and maximum trust, respectively. Each follower i can obtain state information from any neighbor j through communication and sensing, where the redundancy in state information is used to compute τ_{ij}. Let $x_{i,1} : [0,\infty) \to \mathbb{R}^n$ and $x_{i,2} : [0,\infty) \to \mathbb{R}^n$ denote the communicated and sensed, i.e., measured, state of follower i, respectively. Subscripts 1 and 2 denote the type of data, i.e., 1 refers to communicated data and 2 refers to sensed data, where both types of data describe the same quantity.

Let $\{t_k^j\}_{k=0}^{\infty} \subset \mathbb{R}_{\geq 0}$ be an increasing sequence of event-times determined by the event-trigger mechanism of follower j, where the event-time t_k^j denotes the kth instance of follower j broadcasting its state information to its neighbors, all of which are received simultaneously. Let $t_{\text{reset}} \in \mathbb{R}_{>0}$ be a user-defined parameter that denotes the length of time over which trust is determined. The trust follower i has in neighbor j is determined by (see the motivating result in [17])

$$\tau_{ij}(t) \triangleq \begin{cases} 1, & |S_j| = 0 \\ \frac{1}{|S_j|} \sum\limits_{t_k^j \in S_j} e^{-s_1 \Psi_{ij}(t_k^j)}, & |S_j| \neq 0 \end{cases} \tag{4}$$

$$\Psi_{ij}\left(t_k^j\right) \triangleq \left\| x_{j,1}\left(t_k^j\right) - x_{j,2}\left(t_k^j\right) \right\|$$

where $S_j \triangleq \{t_k^j \in \mathbb{R}_{\geq 0} : t - t_{\text{reset}} \leq t_k^j < t\}$, $x_{j,1}(t_k^j)$ and $x_{j,2}(t_k^j)$ denote the communicated and sensed version of the state of follower j at event-time t_k^j, respectively, and $s_1 \in \mathbb{R}_{>0}$ is a user-defined parameter that determines how fast trust decreases. Note that $\Psi_{ij}(t_k^j)$ measures the discrepancy in the state information follower i has about follower $j \in \mathcal{N}_i(t)$ at time t_k^j. Other trust models can be used instead of (4) provided agreement and disagreement between the communicated and sensed version of the state of follower j results in high and low trust, respectively. In (4), all agents begin with maximum trust. However, as discrepancies in the two-point authentication of follower j grow, the trust value of follower j decreases to zero. Conversely, the trust of follower j may increase given the discrepancies in the two-point authentication of follower j are negligible for each $t_k^j \in S_j$, i.e., if $\Psi_{ij}(t_k^j) \approx 0$ for each $t_k^j \in S_j$, then $\tau_{ij}(t) \approx 1$. In the event that follower $j \in \mathcal{N}_i(t)$ does not provide state information to follower i when required, i.e., $\Delta t_k^j \triangleq t_k^j - t_{k-1}^j > \Delta_j$, then $\Psi_{ij}(t_k^j) = \vartheta$, where $\Delta_j \in \mathbb{R}_{>0}$ is a user-defined parameter based on either a simulation/experimental study or an analysis-based derivation, and $\vartheta \in \mathbb{R}_{>0}$ is a user-defined penalty. Similarly, if the distance between follower $j \in \mathcal{N}_i(t)$ and follower i is beyond a user-defined threshold a time t_k^j, i.e., $r < \omega_{ij}(t_k^j) \triangleq \|x_i(t_k^j) - x_{j,2}(t_k^j)\| \leq R$, for $r \in (0, R)$, then $\Psi_{ij}(t_k^j) = \vartheta$.

Remark 2: Assumption 7 affords each agent access to ground-truth state information for each of its neighbors, where comparisons between the communicated and sensed states enable Type I Byzantine agent detection. Moreover, Type II Byzantine agents can abandon the MAS while potentially communicating true state information that could pull the remaining agents with them in their attempt to maintain connectivity. Such a scenario may perturb and destabilize the MAS. Therefore, agent i requires access to accurate state information for each $j \in \mathcal{N}_i(t)$ that is $r-$close to $x_i(t)$ to ensure Type I and Type II Byzantine agent detection for each $i \in \mathcal{V}$.

Remark 3: By Assumption 7, follower i is able to measure the state of follower $j \in \mathcal{N}_i(t)$ each time follower j broadcasts its state. Therefore, Assumption 7 implies that the broadcast state of follower j is synchronized with the measured state of follower j. In practice, achieving synchronization between the broadcast and sensed states of follower j may be unattainable, where the sensed state may be obtained $\delta t > 0$ time units after the broadcast state is received. However, the s_1 parameter in (4) can be tuned to account for the asynchronous state information provided $\delta t > 0$ is small enough, such that $\|x_{j,1}(t_k^j) - x_{j,2}(t_k^j + \delta t)\| \leq \epsilon(\delta t)$ for small $\epsilon(\delta t) > 0$. Future works aim at developing trust models that enable Byzantine agent detection through the use of asynchronous state information, where [20] and [21] serve as potential inroads.

B. Reputation Model

Because a Byzantine agent can provide different state information to each of its neighbors, each neighbor may have a different trust value for the same Byzantine agent. However, multiple trust values for a common neighbor can be consolidated into an overall reputation for the common neighbor. Let $\mathcal{N}_{ij}(t) \triangleq \mathcal{N}_i(t) \cap \mathcal{N}_j(t)$ denote the set of common neighbors shared between followers i and j. Motivated by [17], the continuous reputation $\zeta_{ij} : [0,\infty) \to \mathbb{R}_{\geq 0}$ follower i has for follower $j \in \mathcal{N}_i(t)$ is

$$\dot{\zeta}_{ij}(t) \triangleq \operatorname{proj}\Bigg(\eta_\tau \left(\tau_{ij}(t) - \zeta_{ij}(t)\right) + \sum_{n \in \mathcal{N}_{ij}(t)} \eta_\zeta \zeta_{in}(t) \left(\zeta_{nj}\left(t_k^n\right) - \zeta_{ij}(t)\right) \Bigg) \tag{5}$$

where $\zeta_{ij}(0) = 1$ and $\text{proj}(\cdot)$ denotes the continuous projection operator defined in [22] that is used to ensure $\zeta_{ij}(t) \in [0, 1]$ for all $t \geq 0$. In (5), the parameters $\eta_\tau \in \mathbb{R}_{>0}$ and $\eta_\zeta \in \mathbb{R}_{>0}$ allow the user to select whether the reputation model places more emphasis on measured information, i.e., $\tau_{ij}(t) - \zeta_{ij}(t)$; observed information, i.e., $\zeta_{in}(t)(\zeta_{nj}(t_k^n) - \zeta_{ij}(t))$; or weighs both measured and observed information equally.

Like the trust model in (4), reputation values of 0 and 1 correspond to no and maximum reliability, respectively. At event-time t_k^n, follower i receives reputation values held by follower $n \in \mathcal{N}_i(t)$ for all followers $j \in \mathcal{N}_n(t)$, i.e., $\zeta_{nj}(t_k^n)$, where follower i computes $\zeta_{in}(t)(\zeta_{nj}(t_k^n) - \zeta_{ij}(t))$ over $n \in \mathcal{N}_{ij}(t)$. The measured information in (5) contributes toward the reputation held by follower i for follower j based on the trust measurements follower i has of follower j. The observed information in (5) contributes to the reputation held by follower i for follower j based on the reputation of follower j held by common neighbors $n \in \mathcal{N}_{ij}(t)$, which is weighted based on the corresponding reputation of follower $n \in \mathcal{N}_{ij}(t)$. Hence, a common neighbor $n_1 \in \mathcal{N}_{ij}(t)$ with a low reputation has less influence on the reputation of neighbor j than common neighbor $n_2 \in \mathcal{N}_{ij}(t) \setminus \{n_1\}$ with a higher reputation.

C. Edge Weight Policy

The edge weights of $\mathcal{G}(t)$ encode the degree of influence each neighbor $j \in \mathcal{N}_i(t)$ has on follower i. Since the objective is to achieve FCLT by the cooperative followers, and the reputation model captures the degree of reliability of each follower, the edge weights can be continuously updated according to the reputation model. The edge weight $a_{ij}(t)$ is defined by

$$a_{ij}(t) \triangleq \begin{cases} \zeta_{ij}(t), & \zeta_{ij}(t) \geq \zeta_{\min} \text{ and } j \in \mathcal{N}_i(t) \\ 0, & \zeta_{ij}(t) < \zeta_{\min} \text{ or } j \notin \mathcal{N}_i(t) \end{cases}, \tag{6}$$

where $\zeta_{\min} \in [0, 1]$ is a user-defined parameter that determines whether follower i categorizes follower $j \in \mathcal{N}_i(t)$ as cooperative or Byzantine.

The set of cooperative and Byzantine neighbors of follower i at time t are given by $\mathcal{C}_i(t) \triangleq \{j \in \mathcal{N}_i(t) : a_{ij}(t) \neq 0\}$ and $\mathcal{B}_i(t) \triangleq \mathcal{N}_i(t) \setminus \mathcal{C}_i(t)$, respectively. Remark 4 explains the time-varying nature of the cooperative and Byzantine neighbor sets. Furthermore, $\mathcal{B}(t) \triangleq \{j \in \mathcal{V} : j \in \mathcal{B}_i(t) \text{ for some } i \in \mathcal{V}\}$ and $\mathcal{C}(t) \triangleq \mathcal{V} \setminus \mathcal{B}(t)$. From (6), the edge weight $a_{ij}(t)$ is positive if follower j is a cooperative neighbor of follower i. Conversely, edge weight $a_{ij}(t)$ is zero if followers i and j are not neighbors or if follower j is a Byzantine neighbor of follower i. Note that if $j \in \mathcal{B}_i(t)$, then follower j cannot influence follower i. However, follower i can still compute trust and reputation for follower $j \in \mathcal{N}_i(t)$, where follower j can be reintegrated into $\mathcal{C}_i(t)$ once $\zeta_{ij}(t) \geq \zeta_{\min}$ provided $j \in \mathcal{N}_i(t)$. This enables a remediated Byzantine agent to enter the CMAS and become cooperative neighbors with any cooperative agent. Hence, the information exchange and influence between agents are decoupled. Furthermore, if follower $j \in \mathcal{B}_i(t)$, then follower i will not communicate any true state information about itself to follower j until follower j becomes a cooperative neighbor of follower i. Note that the leader will only communicate state information to its cooperative neighbors by also using (6). Hence, cooperative state information is only communicated between cooperative agents.

Remark 4: The cooperative and Byzantine neighbor sets are time-varying because cooperative agents may be attacked within contested environments and converted into Byzantine agents. Moreover, it may be possible for operators to employ countermeasures to convert Byzantine agents back into cooperative agents. Hence, a follower may be initiated as cooperative, eventually become Byzantine, and then eventually become cooperative again. While the Byzantine neighbor set of a follower may be empty at some time, Assumption 8 ensures the cooperative neighbor set of each cooperative follower is never empty. This also implies that each cooperative agent cannot have all neighbors be Byzantine if there are at least two cooperative followers in the network. Relaxing Assumption 8 is the subject of future work.

D. Event-Triggered Control Development

The state estimate of agent $i \in \mathcal{V} \cup \{0\}$, which is synchronized among all agents $j \in \mathcal{N}_i(t) \cup \{i\}$, is generated by the zero-order hold

$$\hat{x}_i(t) \triangleq x_{i,1}\left(t_k^i\right), t \in \left[t_k^i, t_{k+1}^i\right). \tag{7}$$

According to (7), agent i samples its position at time t_k^i and broadcasts it to all agents $j \in \mathcal{N}_i(t)$. Each agent $j \in \mathcal{N}_i(t) \cup \{i\}$ equates the state estimate of agent i, i.e., $\hat{x}_i(t)$, to $x_i(t_k^i)$ for all time until the next broadcast event of agent i. Recall that $x_{i,1}(t)$ denotes the broadcast state of agent i at time t, which cooperative agents communicate accurately, i.e., $x_{i,1}(t_k^i) = x_i(t_k^i)$. Based on the subsequent stability analysis, the controller for follower $i \in \mathcal{V}$ is

$$u_i(t) \triangleq g_i^+\left(x_i(t)\right)\left(k_1 z_i(t) + k_2 e_{2,i}(t)\right) \tag{8}$$

$$z_i(t) \triangleq \sum_{j \in \mathcal{N}_i(t)} a_{ij}(t)\left(\hat{x}_j(t) - \hat{x}_i(t) - v_j + v_i\right) + b_i(t)\left(v_i + \hat{x}_0(t) - \hat{x}_i(t)\right), \tag{9}$$

where

$$k_1 \triangleq \frac{1}{\Lambda_{\min}}\left(k_{1,1} + \frac{\rho_1^2}{\delta_1}\right) \in \mathbb{R}_{>0},$$

$k_2 \triangleq k_{2,1} + \frac{\rho_2^2}{\delta_2} \in \mathbb{R}_{>0}$, $k_{1,1} \triangleq k_{1,2} + k_{1,3} \in \mathbb{R}_{>0}$, and $k_{1,2}, k_{1,3}, k_{2,1}, \rho_1, \rho_2, \delta_1, \delta_2 \in \mathbb{R}_{>0}$ are parameters defined in Theorem 1. Note that $\Lambda_{\min} \in \mathbb{R}_{>0}$ is a parameter defined in Lemma 2, and $z_i : [0, \infty) \to \mathbb{R}^n$ is the estimate-based distributed FCLT control effort. The stacked form of (9) is defined by $Z \triangleq [z_1^\top(t), z_2^\top(t), \ldots, z_N^\top(t)]^\top \in \mathbb{R}^{nN}$.

The stacked error systems for the leader–follower relative position error in (2) and state estimation error in (3) are $E_1 \triangleq [e_{1,1}^\top(t), e_{1,2}^\top(t), \ldots, e_{1,N}^\top(t)]^\top \in \mathbb{R}^{nN}$ and $E_2 \triangleq [e_{2,1}^\top(t), e_{2,2}^\top(t), \ldots, e_{2,N}^\top(t)]^\top \in \mathbb{R}^{nN}$, respectively. Substituting (1)–(3), (8), and (9) into the time-derivative of (2) yields

$$\dot{e}_{1,i}(t) = f_i\left(x_i(t)\right) + k_1 \sum_{j \in \mathcal{N}_i(t)} a_{ij}(t)\left(e_{2,j}(t) - e_{2,i}(t)\right)$$

$$+ k_1 \sum_{j\in\mathcal{N}_i(t)} a_{ij}(t)\left(e_{1,j}(t) - e_{1,i}(t)\right) + k_1 b_i(t) e_{2,0}(t)$$
$$- k_1 b_i(t) e_{1,i}(t) - k_1 b_i(t) e_{2,i}(t) + k_2 e_{2,i}(t) + d_i(t)$$
$$- \dot{x}_0(t). \tag{10}$$

Substituting (1)–(3), and (7)–(9) into the time-derivative of (3) yields

$$\dot{e}_{2,i}(t) = -f_i\left(x_i(t)\right) - k_1 \sum_{j\in\mathcal{N}_i(t)} a_{ij}(t)\left(e_{2,j}(t) - e_{2,i}(t)\right)$$
$$- k_1 \sum_{j\in\mathcal{N}_i(t)} a_{ij}(t)\left(e_{1,j}(t) - e_{1,i}(t)\right) - k_1 b_i(t) e_{2,0}(t)$$
$$+ k_1 b_i(t) e_{1,i}(t) + k_1 b_i(t) e_{2,i}(t) - k_2 e_{2,i}(t) - d_i(t). \tag{11}$$

Substituting (10) and (11) into the time-derivative of E_1 and E_2, respectively, and compactly expressing the results with the Kronecker product yields

$$\dot{E}_1 = \widetilde{N} + N_d - k_1\left(H(t)\otimes I_n\right)E_2 - k_1\left(H(t)\otimes I_n\right)E_1$$
$$+ k_1\left(B(t)1_N \otimes e_{2,0}(t)\right) + k_2 E_2 \tag{12}$$

$$\dot{E}_2 = -F(X) + k_1\left(H(t)\otimes I_n\right)E_2 + k_1\left(H(t)\otimes I_n\right)E_1$$
$$- k_1\left(B(t)1_N \otimes e_{2,0}(t)\right) - k_2 E_2 - D, \tag{13}$$

where $\widetilde{N} \triangleq F(X) - F(X_0) \in \mathbb{R}^{nN}$, $N_d \triangleq F(X_0) + D - \dot{X}_0 \in \mathbb{R}^{nN}$, $F(X) \triangleq [f_1^\top(x_1(t)), f_2^\top(x_2(t)), \ldots, f_N^\top(x_N(t))]^\top \in \mathbb{R}^{nN}$, $F(X_0) \triangleq [f_1^\top(x_0(t)), f_2^\top(x_0(t)), \ldots, f_N^\top(x_0(t))]^\top \in \mathbb{R}^{nN}$, $D \triangleq [d_1^\top(t), d_2^\top(t), \ldots, d_N^\top(t)]^\top \in \mathbb{R}^{nN}$, $X_0 \triangleq 1_N \otimes x_0(t) \in \mathbb{R}^{nN}$, $X \triangleq [x_1^\top(t), x_2^\top(t), \ldots, x_N^\top(t)]^\top \in \mathbb{R}^{nN}$, and $\mathbf{V} \triangleq [v_1^\top, v_2^\top, \ldots, v_N^\top]^\top \in \mathbb{R}^{nN}$. Given the dynamics in (1) and Assumptions 1–3, and 6, there exists a $c_1 \in \mathbb{R}_{>0}$, such that $\|N_d\| \le c_1$. By Assumption 3, there exists a $c_2 \in \mathbb{R}_{>0}$, such that $\|D\| \le c_2$. By Assumptions 1 and 6, there exists a $c_3 \in \mathbb{R}_{>0}$, such that $\|F(X_0)\| \le c_3$. Using Assumption 9, there exists a $c_4 \in \mathbb{R}_{>0}$, such that $\|\mathbf{V}\| \le c_4$. Using [23, Lemma 5], we can bound $\widetilde{N}$ as $\|\widetilde{N}\| \le \mu(\|E\|)\|E\| + c_5$, where $E(t) \triangleq [E_1^\top, E_2^\top]^\top \in \mathbb{R}^{2nN}$ denotes the MAS error, $\mu : \mathbb{R}_{\ge 0} \to \mathbb{R}_{\ge 0}$ is a positive, nondecreasing, and radially unbounded function, and $c_5 \in \mathbb{R}_{>0}$ is a bounding constant. Note that $E(0) = [E_1^\top(0), E_2^\top(0)]^\top$, where $E_k(0) = [e_{k,1}^\top(0), e_{k,2}^\top(0), \ldots, e_{k,N}^\top(0)]^\top$ for $k \in \{1, 2\}$.

Recall that the objective is to minimize $e_{1,i}(t)$ as given by (2) for each $i \in \mathcal{C}(t)$. However, E_1 and E_2 may contain error systems belonging to Byzantine agents, which cannot be controlled, may be unbounded, and may prevent the objective. Therefore, the FCLT error and the state estimation error are set to zero for all Byzantine agents, i.e., $e_{1,i}(t) \triangleq 0_n$ and $e_{2,i}(t) \triangleq 0_n$ for all $i \in \mathcal{B}(t)$, which allows the objective to apply only to the cooperative followers.

VI. Stability Analysis

To facilitate the subsequent stability analysis, consider the following lemmas.

Lemma 1: There exists a bounding constant $\Lambda_{\max} \in \mathbb{R}_{>0}$, such that $\|H(t)\otimes I_n\| \le \Lambda_{\max}$ for all $t \ge 0$.

Proof: See Appendix A.

Lemma 2: If Assumptions 4, 7, and 8 are satisfied for all $t \ge 0$, then a bounding constant $\Lambda_{\min} \in \mathbb{R}_{>0}$ exists, such that $E_1^\top(H(t)\otimes I_n)E_1 \ge \Lambda_{\min}\|E_1\|^2$ for all $t \ge 0$.[4]

Proof: See Appendix B.

Furthermore, consider the following. Substituting (2), (3), and (9) for all $i \in \mathcal{V}$ into Z yields

$$Z = -\left(H(t)\otimes I_n\right)E_1 - \left(H(t)\otimes I_n\right)E_2$$
$$+ \left(B(t)1_N \otimes e_{2,0}(t)\right). \tag{14}$$

Using Lemma 1, (14), and Young's inequality, it follows that:

$$-k_{1,3}\|E_1\|^2 \le k_{1,3}\|E_2\|^2 - \frac{k_{1,3}}{(2\Lambda_{\max}^2 + \Lambda_{\max})}\|Z\|^2$$
$$+ \frac{k_{1,3}}{\Lambda_{\max}}\|B(t)1_N \otimes e_{2,0}(t)\|^2. \tag{15}$$

Note that (15) is a useful inequality that facilitates the development of the event-trigger mechanisms for the leader and the followers. Moreover, observe that

$$\|B(t)1_N \otimes e_{2,0}(t)\|^2 \le N b_{\max}^2 \|e_{2,0}(t)\|^2 \tag{16}$$

since $\|B(t)1_N \otimes e_{2,0}(t)\|^2 = \sum_{i\in\mathcal{V}} b_i^2(t)\|e_{2,0}(t)\|^2$ and $b_i(t) \in [0, b_{\max}]$ for all $t \ge 0$ and each $i \in \mathcal{V}$ by construction. The subsequent stability analysis uses several auxiliary parameters. Let

$$\phi_1 \triangleq \left(1 - \frac{1}{\kappa}\left(\frac{2\Lambda_{\max}+1}{2\Lambda_{\min}}\right)\right)k_{1,2} - \frac{1}{2}$$
$$- \frac{1}{\kappa}\left(k_{1,3} + \frac{\rho_1^2}{\delta_1}\right)\left(\frac{2\Lambda_{\max}+1}{2\Lambda_{\min}}\right) - \frac{k_2}{2\kappa},$$
$$\phi_2 \triangleq k_{2,1} - \frac{1}{2}, \quad \phi_3 \triangleq \frac{k_1}{2} + \frac{\kappa k_1}{2} + \frac{k_{1,3}}{\Lambda_{\max}},$$
$$\phi_4 \triangleq \frac{k_1}{2} + k_{1,3} + k_1\Lambda_{\max} + \frac{\kappa\left(2k_1\Lambda_{\max} + k_2\right)}{2},$$
$$\phi_5 \triangleq \frac{k_{1,3}}{(2\Lambda_{\max}^2 + \Lambda_{\max})}, \quad \phi_6 \triangleq \min\{\phi_1, \phi_2\},$$
$$\delta^* \triangleq \delta_1 + \delta_2 + c_0 + \varepsilon. \tag{17}$$

Note that κ, c_0, and ε are defined in Theorem 1. The set over which the stability analysis is performed is

$$\mathcal{D} \triangleq \left\{\xi \in \mathbb{R}^{2nN} : \|\xi\| < \inf \mu^{-1}\left(\left[\sqrt{\phi_6/4}, \infty\right)\right)\right\},$$

where, given a set $\Omega \subset \mathbb{R}$, the preimage $\mu^{-1}(\Omega) \subset \mathbb{R}$ is defined as $\mu^{-1}(\Omega) \triangleq \{\omega \in \mathbb{R} : \mu(\omega) \in \Omega\}$. The admissible set of initial conditions is

$$\mathcal{S}_{\mathcal{D}} \triangleq \left\{\xi \in \mathbb{R}^{2nN} : \|\xi\| < \frac{\sqrt{2}}{2}\inf \mu^{-1}\left(\left[\sqrt{\phi_6/4}, \infty\right)\right)\right\}.$$

[4]The use of Assumption 7 the trust model in (4), reputation model in (5), and edge weight policy in (6) ensure Type I and Type II Byzantine agents are detected and removed from the CMAS.

Let $E_{\max} \triangleq \frac{\sqrt{2}}{2}\inf \mu^{-1}([\sqrt{\phi_6/4},\infty))$, and recall that μ is a nondecreasing function. If $\|E\| < E_{\max}$, then $\mu(\|E\|) \leq \sqrt{\phi_6/4}$. In the Appendix, we present an algorithm that summarizes the control strategy used by each agent to achieve the objective. The algorithm is expressed with respect to follower i, and a similar algorithm follows for the leader. Recall that $\omega_{ij}(t_k^j) = \|x_i(t_k^j) - x_{j,2}(t_k^j)\|$ and $\Delta t_k^j = t_k^j - t_{k-1}^j$ as defined in Section V-A.

Theorem 1: The trust model in (4), reputation model in (5), edge weight policy in (6), estimator in (7), and controller in (8) and (9) ensure the MAS error E is uniformly ultimately bounded (UUB) in the sense that

$$\mathit{lim\ sup}_{t\to\infty} \|E\| \leq 2\sqrt{\frac{4c_5^2 + 2\delta^*}{\phi_6}} \tag{18}$$

provided the leader broadcasts its state as dictated by the event-trigger mechanism in

$$t_{k+1}^0 \triangleq \inf\left\{t > t_k^0 : Nb_{\max}^2\phi_3\left\|e_{2,0}(t)\right\|^2 \geq c_0\right\}, \tag{19}$$

each follower $i \in \mathcal{V}$ broadcasts its state as dictated by the event-trigger mechanism in

$$t_{k+1}^i \triangleq \inf\left\{t > t_k^i : \phi_4\left\|e_{2,i}(t)\right\|^2 \geq \phi_5\left\|z_i(t)\right\|^2 + \frac{\varepsilon}{N}\right\}, \tag{20}$$

Assumptions 1–9 are satisfied, the initial condition of the system is selected, such that $E(0) \in \mathcal{S}_{\mathcal{D}}$, and the following sufficient user-defined parameter conditions are satisfied:

$$\kappa > \frac{2\Lambda_{\max}+1}{2\Lambda_{\min}},\ \ k_{1,3} > 0,\ \ k_{2,1} > \frac{1}{2},\ \ \rho_1 \geq c_1,$$
$$\rho_2 \geq c_2 + c_3,\ \ c_0 > 0,\ \ \delta_1 > 0,\ \ \delta_2 > 0,\ \ \varepsilon > 0,$$
$$k_{1,2} > \frac{2\kappa\Lambda_{\min}}{2\left(\kappa\Lambda_{\min} - \Lambda_{\max}\right) - 1}\left(\frac{1}{2} + \frac{k_2}{2\kappa} + \frac{1}{\kappa}\left(k_{1,3} + \frac{\rho_1^2}{\delta_1}\right)\left(\frac{2\Lambda_{\max}+1}{2\Lambda_{\min}}\right)\right),$$

$$\sqrt{\left(8c_5^2 + 4\delta^*\right)/\phi_6} < \frac{\sqrt{2}}{2}\inf\mu^{-1}\left(\left[\sqrt{\phi_6/4},\infty\right)\right). \tag{21}$$

Proof: Consider the candidate Lyapunov function $V_1 : \mathcal{D} \to \mathbb{R}_{\geq 0}$ defined as

$$V_1\left(E(t)\right) \triangleq \frac{1}{2}E_1^\top E_1 + \frac{1}{2}E_2^\top E_2, \tag{22}$$

which can be bounded as

$$\alpha_1\left(\|E\|\right) \leq V_1\left(E(t)\right) \leq \alpha_2\left(\|E\|\right), \tag{23}$$

where $\alpha_1,\ \alpha_2 : \mathbb{R}_{\geq 0} \to \mathbb{R}_{\geq 0}$ are user-defined class $\mathcal{K}$ functions. Without loss of generality, let $\alpha_1(\|E\|) \triangleq \frac{1}{2}\|E\|^2$ and $\alpha_2(\|E\|) \triangleq \|E\|^2$. Suppose $g : [0,\infty) \to \mathbb{R}^{2nN}$ is a Filippov solution to the differential inclusion $\dot{g}(t) \in K[h](g(t))$, where $g(t) = E(t)$, the mapping $K[\cdot]$ provides a calculus for computing Filippov's differential inclusion as defined in [24], and $h : \mathbb{R}^{2nN} \to \mathbb{R}^{2nN}$ is defined as $h(g(t)) = [\dot{E}_1^\top, \dot{E}_2^\top]^\top$. The time-derivative of V_1 exists almost everywhere (a.e.), i.e., for almost all $t \in [0,\infty)$, and

$$\dot{V}_1\left(g(t)\right) \overset{a.e.}{\in} \dot{\tilde{V}}_1\left(g(t)\right), \tag{24}$$

where $\dot{\tilde{V}}_1(g(t))$ is the generalized time-derivative of V_1 along the Filippov trajectories of $\dot{g}(t) = h(g(t))$. By [25, eq. 13], $\dot{\tilde{V}}_1(g(t)) \triangleq \bigcap_{\xi\in\partial V_1(g(t))}\xi^\top\left[K[h]^\top(g(t)),\ 1\right]^\top$, where $\partial V_1(g(t))$ denotes the Clarke generalized gradient of $V_1(g(t))$. Since $V_1(g(t))$ is continuously differentiable in $g(t)$, $\partial V_1(g(t)) = \{\nabla V_1(g(t))\}$, where ∇ denotes the gradient operator. The generalized time-derivative of (22) is

$$\dot{\tilde{V}}_1\left(g(t)\right) \subseteq E^\top(t)K\left[h\right]\left(g(t)\right). \tag{25}$$

Using the calculus of $K[\cdot]$ from [24], (25), and simplifying the substitution of (12) and (13) into the generalized time-derivative of (22) yields

$$\begin{aligned}\dot{\tilde{V}}_1\left(g(t)\right) \subseteq &\left\{E_1^\top\widetilde{N} + E_1^\top N_d - E_2^\top F(X) - E_2^\top D\right\}\\ &+ k_1E_2^\top K\left[\left(H(t)\otimes I_n\right)E_2\right] + k_2E_1^\top K\left[E_2\right]\\ &- k_1E_1^\top K\left[\left(H(t)\otimes I_n\right)E_2\right] - k_2E_2^\top K\left[E_2\right]\\ &+ k_1E_2^\top K\left[\left(H(t)\otimes I_n\right)\right]E_1\\ &- k_1E_1^\top K\left[\left(H(t)\otimes I_n\right)\right]E_1\\ &+ k_1E_1^\top K\left[\left(B(t)1_N\otimes e_{2,0}(t)\right)\right]\\ &- k_1E_2^\top K\left[\left(B(t)1_N\otimes e_{2,0}(t)\right)\right],\end{aligned} \tag{26}$$

where set addition is defined by the Minkowski sum. Adding and subtracting $E_2^\top F(X_0)$ and using (24), Lemma 1, Lemma 2, $\|N_d\| \leq c_1, \|D\| \leq c_2,\ \|F(X_0)\| \leq c_3,\ \|\mathbf{V}\| \leq c_4,\ \|\widetilde{N}\| \leq \mu(\|E\|)\|E\| + c_5$, and Young's inequality, (26) can be upper bounded as

$$\begin{aligned}\dot{V}_1\left(E(t)\right) \overset{a.e.}{\leq}\ &\frac{1}{2}\left\|E_1\right\|^2 + 2\mu^2\left(\|E\|\right)\|E\|^2 + 2c_5^2\\ &+ c_1\left\|E_1\right\| + 2k_1\Lambda_{\max}\left\|E_1\right\|\left\|E_2\right\| - k_1\Lambda_{\min}\left\|E_1\right\|^2\\ &+ k_1\left\|E_1\right\|\left\|B(t)1_N\otimes e_{2,0}(t)\right\| + k_2\left\|E_1\right\|\left\|E_2\right\|\\ &+ c_3\left\|E_2\right\| + \frac{1}{2}\left\|E_2\right\|^2 + k_1\Lambda_{\max}\left\|E_2\right\|^2\\ &+ k_1\left\|E_2\right\|\left\|B(t)1_N\otimes e_{2,0}(t)\right\| - k_2\left\|E_2\right\|^2\\ &+ c_2\left\|E_2\right\|.\end{aligned} \tag{27}$$

Since $\rho_1 \geq c_1$ and $\rho_2 \geq c_2 + c_3$ by the hypothesis of Theorem 1, we then see that $(c_1 - \frac{\rho_1^2}{\delta_1}\|E_1\|)\|E_1\| \leq \delta_1$ and $(c_2 + c_3 - \frac{\rho_2^2}{\delta_2}\|E_2\|)\|E_2\| \leq \delta_2$. Using these bounds, $k_1 = \frac{1}{\Lambda_{\min}}(k_{1,1} + \frac{\rho_1^2}{\delta_1})$, $k_{1,1} = k_{1,2} + k_{1,3}$, $k_2 = k_{2,1} + \frac{\rho_2^2}{\delta_2}$, (15), Young's inequality, the inequality in (16), and the auxiliary parameters in (17) and (27) can be upper bounded by

$$\begin{aligned}\dot{V}_1\left(E(t)\right) \overset{a.e.}{\leq} &-\frac{\phi_6}{2}\|E\|^2 - \left(\frac{\phi_6}{2} - 2\mu^2\left(\|E\|\right)\right)\|E\|^2\\ &+ \sum_{i\in\mathcal{V}}\left(\phi_4\left\|e_{2,i}(t)\right\|^2 - \phi_5\left\|z_i(t)\right\|^2 - \frac{\varepsilon}{N}\right)\\ &+ 2c_5^2 + Nb_{\max}^2\phi_3\left\|e_{2,0}(t)\right\|^2 - c_0 + \delta^*,\end{aligned} \tag{28}$$

where satisfying the parameter conditions in (21) ensures $\phi_i > 0$ $\forall i \in \{1, 2, \ldots, 6\}$. Based on (28), the event-trigger mechanism for the leader is given by (19), and the event-trigger mechanism for each follower $i \in \mathcal{V}$ is given by (20). Since each agent provides state feedback according to the event-trigger mechanisms in (19) and (20), (28) can be upper bounded as

$$\dot{V}_1(E(t)) \overset{a.e.}{\leq} -\frac{\phi_6}{2}\|E\|^2 - \left(\frac{\phi_6}{2} - 2\mu^2(\|E\|)\right)\|E\|^2 + 2c_5^2 + \delta^*. \quad (29)$$

Using (23), we see that $\|E\| \leq \alpha_1^{-1}(\alpha_2(\|E\|))$ and $\alpha_2^{-1}(\alpha_1(\|E\|)) \leq \|E\|$, where $\alpha_1^{-1}(\alpha_2(\|E\|)) = \sqrt{2}\|E\|$ and $\alpha_2^{-1}(\alpha_1(\|E\|)) = \frac{\sqrt{2}}{2}\|E\|$ given the selected class $\mathcal{K}$ functions. Note that $\phi_6/2 - 2\mu^2(\|E\|) > 0$ provided $E_{\max} = \frac{\sqrt{2}}{2}\inf \mu^{-1}([\sqrt{\phi_6/4}, \infty)) > \|E\|$. Moreover, $-(\phi_6/4)\|E\|^2 + 2c_5^2 + \delta^* \leq 0$ provided $\|E\| \geq \sqrt{(8c_5^2 + 4\delta^*)/\phi_6}$. It then follows that (29) can be upper bounded as $\dot{V}_1(E(t)) \overset{a.e.}{\leq} -\frac{\phi_6}{4}\|E\|^2$ for all $E_{\max} > \|E\| \geq \sqrt{(8c_5^2 + 4\delta^*)/\phi_6}$. Let $\mathcal{Z} \triangleq \{\xi \in \mathbb{R}^{2nN} : \|\xi\| \geq \sqrt{(8c_5^2 + 4\delta^*)/\phi_6}\}$. Since $\sqrt{(8c_5^2 + 4\delta^*)/\phi_6} < \frac{\sqrt{2}}{2}\inf \mu^{-1}([\sqrt{\phi_6/4}, \infty))$, we then see that $\dot{V}_1(E(t)) \overset{a.e.}{<} 0$ for all $E \in \mathcal{S}_{\mathcal{D}} \cap \mathcal{Z}$. If $E \in \mathcal{S}_{\mathcal{D}} \cap \mathcal{Z}^C$, then $\dot{V}_1(E(t)) \overset{a.e.}{\leq} -\frac{\phi_6}{4}\|E\|^2 + 2c_5^2 + \delta^*$, which may allow $V_1(E(t))$ to grow. However, E will exit $\mathcal{Z}^C$ before exiting $\mathcal{S}_{\mathcal{D}}$, and, therefore, flow into $\mathcal{S}_{\mathcal{D}} \cap \mathcal{Z}$. It then follows that $\mathcal{S}_{\mathcal{D}}$ is forward invariant, where initializing the MAS, such that $E(0) \in \mathcal{S}_{\mathcal{D}}$ ensures E is uniformly ultimately bounded with the ultimate bound presented in (18).

We now show that the state, state estimate, control signal, FCLT error, and state estimation error are bounded for each agent. Since $E \in \mathcal{L}_\infty$, it follows that $E_1 \in \mathcal{L}_\infty$ and $E_2 \in \mathcal{L}_\infty$ given the definition of E. Since $E_1 \in \mathcal{L}_\infty$, $e_{1,i}(t) \in \mathcal{L}_\infty$ for all $i \in \mathcal{V}$ given the definition of E_1. From Assumption 6, $x_0(t) \in \mathcal{L}_\infty$. Since $e_{1,i}(t) \in \mathcal{L}_\infty$, $v_i \in \mathcal{L}_\infty$, and $x_0(t) \in \mathcal{L}_\infty$, (2) implies $x_i(t) \in \mathcal{L}_\infty$ for each $i \in \mathcal{V}$.

Since $E_2 \in \mathcal{L}_\infty$, we also see that $e_{2,i}(t) \in \mathcal{L}_\infty$ for all $i \in \mathcal{V}$ given the definition of E_2. Since $x_i(t) \in \mathcal{L}_\infty$ and $e_{2,i}(t) \in \mathcal{L}_\infty$, (3) implies $\hat{x}_i(t) \in \mathcal{L}_\infty$ for all $i \in \mathcal{V}$. Since $x_0(t) \in \mathcal{L}_\infty$ by Assumption 6, (7) implies $\hat{x}_0(t) \in \mathcal{L}_\infty$. Since $\hat{x}_i(t) \in \mathcal{L}_\infty$ for all $i \in \mathcal{V} \cup \{0\}$, $a_{ij}(t) \in [0, 1]$ for all $t \geq 0$ and each $i, j \in \mathcal{V}$ by construction, $v_i \in \mathcal{L}_\infty$ for all $i \in \mathcal{V}$ by design, and $b_i(t) \in [0, b_{\max}]$ for all $t \geq 0$ and each $i \in \mathcal{V}$ by construction, (9) implies $z_i(t) \in \mathcal{L}_\infty$ for each $i \in \mathcal{V}$. Since $z_i(t) \in \mathcal{L}_\infty$, $e_{2,i}(t) \in \mathcal{L}_\infty$, $x_i(t) \in \mathcal{L}_\infty$, and $g_i^+(x_i(t)) \in \mathcal{L}_\infty$ by Assumption 2, it follows that (8) implies $u_i(t) \in \mathcal{L}_\infty$ for all $i \in \mathcal{V}$. ■

Remark 5: With respect to (21), c_0 is a user-defined parameter that determines the rate at which the leader broadcasts its state to its neighbors. Moreover, c_0 is used to uniformly lower bound the difference between consecutive broadcast events performed by the leader away from zero. Similarly, ε is a user-defined parameter used to uniformly lower bound the difference between consecutive broadcast events for each follower $i \in \mathcal{V}$ away from zero.

Remark 6: Based on the definition of ϕ_1 and ϕ_2 in (17), ϕ_6 can be increased by increasing $k_{1,2}$ and $k_{2,1}$ provided $k_{1,2}$ and κ are selected according to (21). Given $E(0)$, select ϕ_6, such that $E(0) \in \mathcal{S}_{\mathcal{D}}$. Observe that $\sqrt{(8c_5^2 + 4\delta^*)/\phi_6}$ decreases with increasing ϕ_6, where c_5 and δ^* are fixed. Furthermore, since μ is a nondecreasing function, it follows that $\mu^{-1}([\sqrt{\phi_6/4}, \infty))$ is nondecreasing with respect to ϕ_6. Hence, $\sqrt{(8c_5^2 + 4\delta^*)/\phi_6} < \frac{\sqrt{2}}{2}\inf \mu^{-1}([\sqrt{\phi_6/4}, \infty))$ can be satisfied for some ϕ_6.

We now show the event-trigger mechanisms in (19) and (20) are free from Zeno behavior.

Theorem 2: The difference between consecutive broadcast times generated by the event-trigger mechanism of the leader in (19) is uniformly lower bounded by

$$t_{k+1}^0 - t_k^0 \geq \frac{1}{b_{\max}\theta_{0,\max}}\sqrt{\frac{c_0}{N\phi_3}} \quad (30)$$

for all $k \in \mathbb{Z}_{\geq 0}$, where $\theta_{0,\max} \in \mathbb{R}_{>0}$ is a user-defined parameter selected, such that $\|f_0(x_0(t))\| + \|g_0(x_0(t))\|\|u_0(t)\| + \|d_0(t)\| \leq \theta_{0,\max}$.

Proof: See Appendix C. ■

Theorem 3: The difference between consecutive broadcast times generated by the event-trigger mechanism of follower $i \in \mathcal{V}$ in (20) is uniformly lower bounded by

$$t_{k+1}^i - t_k^i \geq \frac{1}{k_2}\ln\left(\frac{k_2}{\theta_{i,\max}}\sqrt{\frac{\varepsilon}{N\phi_4}} + 1\right) \quad (31)$$

for all $k \in \mathbb{Z}_{\geq 0}$, where $\theta_{i,\max} \in \mathbb{R}_{>0}$ is a user-defined parameter selected, such that $\|f_i(x_i(t))\| + k_1\|z_i(t)\| + \|d_i(t)\| \leq \theta_{i,\max}$.

Proof: See Appendix D. ■

VII. Simulation Study

A simulation study is included to validate the developed approach. The simulated MAS consists of five follower agents and a single leader agent. The initial positions of each agent are $x_0(0) = [500,\ 10]^\top$, $x_1(0) = [465, -51]^\top$, $x_2(0) = [566, -52]^\top$, $x_3(0) = [417, -103]^\top$, $x_4(0) = [518, -104]^\top$, and $x_5(0) = [619, -105]^\top$. The uncertain drift dynamics[5] and known control effectiveness matrix of agent i are $f_i(x_i(t)) \triangleq [\bar{a}_{1i}\psi(x_{1i}(t)) + \bar{a}_{2i}, \bar{a}_{3i} + \bar{a}_{4i}\psi(x_{2i}(t))]^\top \in \mathbb{R}^2$ and

$$g_i(x_i(t)) \triangleq \begin{bmatrix} \cos(\varphi_i(t)) & -\sin(\varphi_i(t)) \\ \sin(\varphi_i(t)) & \cos(\varphi_i(t)) \end{bmatrix} \in \mathbb{R}^{2\times 2},$$

respectively, where $x_i(t) \triangleq [x_{1i}(t), x_{2i}(t)]^\top \in \mathbb{R}^2$, $\bar{a}_i \triangleq [\bar{a}_{1i}, \bar{a}_{2i}, \bar{a}_{3i}, \bar{a}_{4i}]^\top \in \mathbb{R}^4$,

$$\psi(x) \triangleq \frac{1}{\sigma\sqrt{2\pi}}\exp\left(-\frac{x^2}{2\sigma^2}\right) \in \mathbb{R}_{>0},$$

and

$$\varphi_i(t) \triangleq \arctan\left(\frac{x_{2i}(t)}{x_{1i}(t)}\right) \in \mathbb{R},$$

such that $\arctan(\cdot)$ is the four quadrant inverse tangent, i.e., `atan2`$(\cdot)$ with respect to MATLAB. The uncertain drift

[5]The leader knows its drift dynamics while the followers do not know their drift dynamics.

dynamics coefficients for each agent are $\bar{a}_0 \triangleq [1,\ 1,\ 1,\ 1]^\top$, $\bar{a}_1 \triangleq [1,\ 1.5,\ 3,\ 2]^\top, \bar{a}_2 \triangleq [0.5,\ 0.5,\ 1.9,\ 0.7]^\top$, $\bar{a}_3 \triangleq [1.5,\ 2.1,\ 1.2,\ 0.5]^\top, \bar{a}_4 \triangleq [3,\ 1.75,\ 1.15,\ 3]^\top$, and $\bar{a}_5 \triangleq [2,\ 1,\ 1,\ 1.6]^\top$. The exogenous disturbance acting on all agents is random, drawn from a normal distribution, and scaled by $d_{\mathrm{mag}} \in \mathbb{R}_{>0}$, which is subsequently defined. The relative position vectors defining the desired formation are $v_1 \triangleq [-50, -50]^\top$, $v_2 \triangleq [50, -50]^\top$, $v_3 \triangleq [-100, -100]^\top$, $v_4 \triangleq [0, -100]^\top$, and $v_5 \triangleq [100, -100]^\top$. The known desired trajectory $x_d : [0, \infty) \to \mathbb{R}^2$ of the leader is $x_d(t) \triangleq 500[\cos(2\pi 10^{-2} t), \sin(2\pi 10^{-2} t)]^\top$, while the leader's trajectory tracking error $e_0 : [0, \infty) \to \mathbb{R}^2$ is defined as $e_0(t) \triangleq x_d(t) - x_0(t)$. The leader's tracking error can be globally exponentially regulated using the following controller: $u_0(t) \triangleq g_0^+(x_0(t))(-f_0(x_0(t)) + \dot{x}_d(t) + k_{0,1} e_0(t) + k_{0,2}\mathrm{sgn}(e_0(t)))$, where $k_{0,1} \in \mathbb{R}_{>0}$ and $k_{0,2} \in \mathbb{R}_{>0}$ are user-defined parameters. The simulation is 50 time units long and uses an integration time-step of 1.00×10^{-3} time units. The following parameters are used to generate the simulation results: $b_{\max} = 1.25$, $\vartheta = 10$, $\sigma = 100$, $R = 110$, $k_{0,1} = 1$, $k_{0,2} = 0.25$, $d_{\mathrm{mag}} = 0.03$, $c_1 = 3$, $c_2 = 1$, $c_3 = 0.008$, $\Lambda_{\min} = 1$, $\Lambda_{\max} = 10$, $\rho_1 = 4$, $\delta_1 = 0.25$, $\rho_2 = 2.008$, $\delta_2 = 0.25$, $\kappa = 105$, $k_{1,3} = 1$, $k_{2,1} = 1$, $k_{1,2} = 15.74$, $\varepsilon = 10^6$, $c_0 = 10^4$, $N = 5$, $s_1 = 5$, $t_{\mathrm{reset}} = 1$, $\Delta_i = 0.125$ for each $i \in \{1, 2, \ldots, 5\}$, $\eta_\tau = 70$, $\eta_\zeta = 70$, and $\zeta_{\min} = 0.95$. The adjacency matrix of the communication graph of the followers and the leader pinning matrix are

$$\mathcal{A} = \begin{bmatrix} 0 & 0 & 1 & 1 & 0 \\ 0 & 0 & 0 & 1 & 1 \\ 1 & 0 & 0 & 1 & 0 \\ 1 & 1 & 1 & 0 & 1 \\ 0 & 1 & 0 & 1 & 0 \end{bmatrix}$$

and $B(t) = b_{\max} \cdot \mathrm{diag}(1,\ 1,\ 0,\ 0,\ 0)$, respectively.

Figs. 1 and 2 display the simulation results. The simulation subjected the MAS to at most two Byzantine agents, where Follower 3 was converted to a Type II Byzantine agent for $t \in [10, 40]$ time units, and Follower 5 was converted to a Type I Byzantine agent for $t \in [13, 40]$ time units. Follower 3 does not communicate with its neighbors during $t \in [10, 40]$. For $t \in [10, 30]$, Follower 3 was first maneuvered to $[225,\ 150]$ in an attempt to strain the network and destabilize the CMAS. For $t \in [30, 40]$, Follower 3 was maneuvered toward the CMAS, where it was converted back to a cooperative follower for $t > 40$ time units.[6]

The controller used to maneuver Follower 3 to $[225,\ 150]$ and then back to the CMAS is identical in form to that of the leader, where exact model knowledge was used only for the purpose of moving the follower away from the CMAS and simulating unanticipated behavior of an initial member of the CMAS. The communication protocol used by Follower 5 during $t \in [13, 40]$ was $x_{5,1}(t) = -0.1 \cdot x_5(t)$, i.e., the communicated information was negative one-tenth the true state of Follower 5. Since Follower 5 remained with the CMAS for $t \in [13, 40]$, its tracking error $e_{1,5}(t)$ is similar to that of the cooperative followers.

The cooperative followers, i.e., Followers 1, 2, and 4, satisfied the objective for all time, even in the presence of the Byzantine

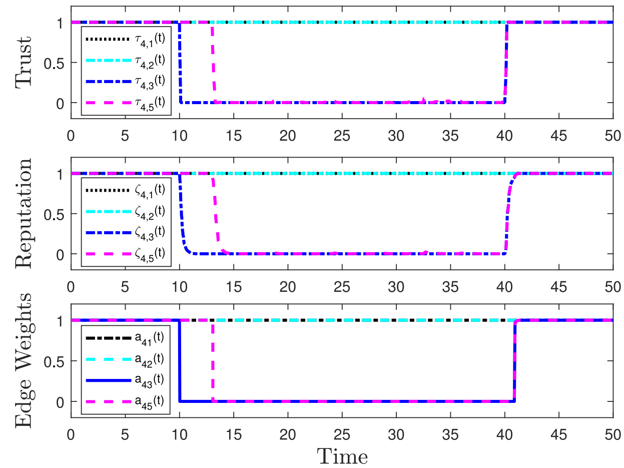

Fig. 1. Trust, reputation, and edge weight values that Follower 4 has for its neighbors. Since Followers 1 and 2 are cooperative agents for all time, they communicate true state information about themselves to Follower 4, which results in maximum trust, reputation, and edge weight values for all time. Conversely, Followers 3 and 5 are Byzantine for $t \in [10, 40]$ and $t \in [13, 40]$, respectively, which results in their zero trust, reputation, and edge weight values with respect to Follower 4 during their Byzantine status. The trust, reputation, and edge weight values that Follower 4 has in Followers 3 and 5 are quickly restored to the maximum once Followers 3 and 5 become cooperative for $t > 40$ and $t > 40$, respectively.

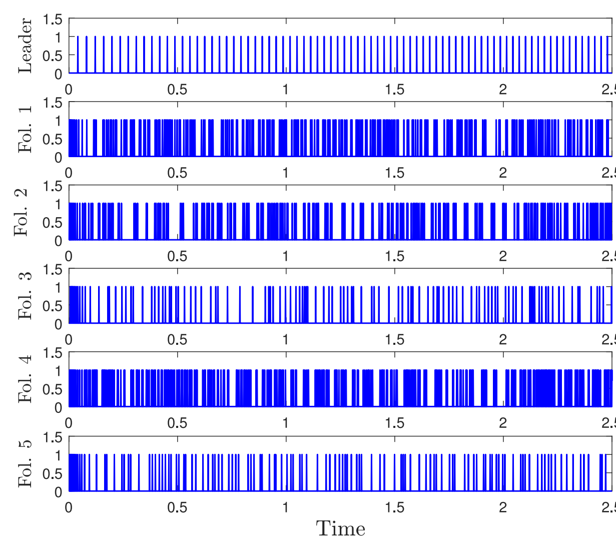

Fig. 2. Illustration of event-times for the leader and each follower during the first 2.5 time units of the simulation. A 0 or white space, denotes no communication and 1, or blue line, denotes a communication event. The first 2.5 time units of the simulation are shown, rather than entire simulation, to better exhibit the intermittency in communication.

[6]An adversary may corrupt a cooperative agent and cause it to abandon the CMAS. However, it may be possible to execute countermeasures to convert the Byzantine agent back into a cooperative agent. In such a case, it may be desirable to maneuver the cooperative agent back into the formation formed by the remaining cooperative agents.

adversaries. Followers 3 and 5 also satisfied the objective during their periods of cooperation. Fig. 1 depicts the trust, reputation, and edge weights of the neighbors of Follower 4, which illustrates the Byzantine behavior of Followers 3 and 5. The trust, reputation, and edge weight figures for Followers 1, 2, 3, and 5 are omitted since they are similar to those of Follower 4. Fig. 1 shows that Follower 4 detected the Byzantine behavior of Followers 3 and 5 at $t = 10$ and $t = 13$, respectively. As a result of the detected Byzantine behavior, the trust that Follower 4 had in Followers 3 and 5 decreased to 0, which caused the corresponding reputation values and edge weights to decrease to 0. Fig. 1 shows that Follower 4 detected cooperative behavior from Followers 3 and 5 at $t > 40$ and $t > 40$, respectively, which caused the trust, reputation, and edge weights of Followers 3 and 5 with respect to Follower 4 to increase to 1.

Fig. 2 depicts the event-times for the leader and each follower for the first 2.5 time units of the simulation. The average differences between consecutive event-times for the entire simulation for the leader and Followers 1–5 are 0.0282, 0.0144, 0.0136, 0.0016, 0.0141, and 0.0197 time units, respectively. The minimum differences between consecutive event-times for the leader and Followers 1–5 are 0.028, 0.002, 0.002, 0.001, 0.003, and 0.003 time units, respectively.

VIII. Conclusion

This work examines the formation control while leader tracking problem for a heterogeneous MAS consisting of agents with uncertain nonlinear dynamics. A distributed event-triggered controller is developed along with a reputation-based detection method that enables each follower to discern between cooperative and Byzantine neighbors. The edge weight policy alters the interaction among agents to enable the cooperative followers to achieve the objective. Future efforts will focus on developing controllers capable of ensuring the connectivity of the CMAS and collision avoidance while also considering time-varying formations. Moreover, more sophisticated Byzantine agent detectors that relax Assumption 7 and provide detection guarantees are motivated. While we study the fundamental case of multiple Byzantine adversaries that act independently within this work, future efforts are motivated to examine the case, where multiple Byzantine adversaries collaborate between each other to thwart the objective. Several open questions still remain. For example, how can accurate state information be determined in the absence of a ground-truth? Moreover, for agents with multiple common neighbors and no available ground-truth information, how can an agent determine its cooperative neighbor set if both the true cooperative neighbor set and the true Byzantine neighbor set seem cooperative?

Appendix

A. Proof of Lemma 1

Proof: Let $\mathcal{H} \triangleq \{\|H(t) \otimes I_n\| : t \geq 0\}$. Fix $t_1 \geq 0$, and suppose $\mathcal{C}(t_1) = \mathcal{V}$, $\mathcal{G}(t_1)$ is complete, and $B(t) = b_{\max} \cdot I_N$. Then, $\|H(t) \otimes I_n\|_F$ is maximum at t_1, where $\Lambda_{\max} \triangleq \sqrt{n(N(N-1+b_{\max})^2 + N^2 - N)} = \|H(t_1) \otimes I_n\|_F$. Since $\|H(t) \otimes I_n\| \leq \|H(t) \otimes I_n\|_F \leq \Lambda_{\max}$ for all $t \geq 0$, $\mathcal{H}$ is a nonempty set that is bounded above. Therefore, $\Lambda_{\max} \geq \sup\{\mathcal{H}\}$.

B. Proof of Lemma 2

Proof: Fix $t_2 \geq 0$, and suppose that at time t_2 the MAS consists of $N_C(t_2) \in \mathbb{Z}_{\geq 0}$ cooperative followers and $N_B(t_2) \in \mathbb{Z}_{\geq 0}$ Byzantine adversaries, where $N_C(t_2) + N_B(t_2) = N$. Using Assumptions 4 and 7, the trust model in (4), the reputation model in (5), and the edge weight policy in (6), the connectivity matrix $\overline{H}(t_2)$ can be expressed as the block matrix

$$\overline{H}(t_2) = \begin{bmatrix} H_{CC}(t_2) & H_{CB}(t_2) \\ H_{BC}(t_2) & H_{BB}(t_2) \end{bmatrix},$$

where $H_{CC}(t_2) \in \mathbb{R}^{N_C(t_2) \times N_C(t_2)}$ is a diagonally dominant matrix with positive diagonal entries by construction, $H_{BB}(t_2) \in \mathbb{R}^{N_B(t_2) \times N_B(t_2)}$, $H_{BC}(t_2) \in \mathbb{R}^{N_B(t_2) \times N_C(t_2)}$, and $H_{CB}(t_2) \in \mathbb{R}^{N_C(t_2) \times N_B(t_2)}$. Note that $\overline{H}(t_2) = P(t_2)H(t_2)P^{-1}(t_2)$, where $\overline{H}(t_2)$ is permutation-similar to $H(t_2)$, and $P(t_2)$ is an orthogonal permutation matrix. Since $H_{CC}(t_2)$ is irreducibly diagonally dominant by Assumption 8, $H_{CC}(t_2)$ is nonsingular, i.e., $H_{CC}(t_2)$ is invertible [26, Corollary 6.2.27].[7]

Next, we show that the eigenvalues of $H_{CC}(t_2)$ have positive real parts. Since $P(t_2)$ is orthogonal, $P(t_2)$ is invertible, where $P^{-1}(t_2) = P^\top(t_2)$. Let $\overline{E}_1 \triangleq (P(t_2) \otimes I_n)E_1 \in \mathbb{R}^{nN}$, where $\overline{E}_1 \triangleq [E_{1,C}^\top, E_{1,B}^\top]^\top \in \mathbb{R}^{nN}$, such that $E_{1,C} \triangleq [e_{1,1}^\top(t_2), e_{1,2}^\top(t_2), \ldots, e_{1,N_C(t_2)}^\top(t_2)]^\top \in \mathbb{R}^{nN_C(t_2)}$ and $E_{1,B} \triangleq [e_{1,N_C(t_2)+1}^\top(t_2), e_{1,N_C(t_2)+2}^\top(t_2), \ldots, e_{1,N}^\top(t_2)]^\top = 0_{nN_B(t_2)}$ by convention. Substituting $\overline{H}(t_2)$ and $\overline{E}_1$ into $E_1^\top(H(t_2) \otimes I_n)E_1$ yields $E_1^\top(H(t_2) \otimes I_n)E_1 = E_{1,C}^\top(H_{CC}(t_2) \otimes I_n)E_{1,C}$. Let $H_{\text{sym}}(t_2) \triangleq \frac{1}{2}(H_{CC}(t_2) + H_{CC}^\top(t_2))$ and $H_{\text{skew}}(t_2) \triangleq \frac{1}{2}(H_{CC}(t_2) - H_{CC}^\top(t_2))$, where $H_{\text{sym}}(t_2)$ and $H_{\text{skew}}(t_2)$ are symmetric and skew-symmetric matrices, respectively, by construction. Moreover, $H_{CC}(t_2) = H_{\text{sym}}(t_2) + H_{\text{skew}}(t_2)$. Since $H_{\text{skew}} \otimes I_n$ is a skew-symmetric matrix, $E_{1,C}^\top(H_{\text{skew}}(t_2) \otimes I_n)E_{1,C} = 0$ and $E_{1,C}^\top(H_{CC}(t_2) \otimes I_n)E_{1,C} = E_{1,C}^\top(H_{\text{sym}}(t_2) \otimes I_n)E_{1,C}$. Since $H_{CC}(t_2)$ is a diagonally dominant matrix with positive diagonal entries, the real part of the eigenvalues of $H_{CC}(t_2)$ are nonnegative by the Gershgorin disk theorem in [27, The. 3.9.]. Moreover, since the real part of the eigenvalues of $H_{CC}(t_2)$ are nonnegative and $H_{CC}(t_2)$ is invertible, the real part of the eigenvalues of $H_{CC}(t_2)$ are positive.

We next show that the symmetric component of $H_{CC}(t_2)$ is positive definite. Since $H_{CC}(t_2)$ is invertible, for all nonzero $w \in \mathbb{R}^{N_C(t_2)}$ $H_{CC}(t_2)w \neq 0_{N_C(t_2)}$ and $H_{CC}^\top(t_2)w \neq 0_{N_C(t_2)}$. Moreover, $H_{CC}(t_2)w + H_{CC}^\top(t_2)w \neq 0_{N_C(t_2)}$ since $H_{CC}(t_2) + H_{CC}^\top(t_2) \neq 0_{N_C(t_2) \times N_C(t_2)}$, i.e.,

[7] Every graph Laplacian is diagonally dominant because it has zero row sums. For connected graphs, their Laplacians are irreducible. Adding the Laplacian of a connected graph to a diagonal matrix with at least one positive entry makes at least one row strictly diagonally dominant. Hence, summing a connected graph Laplacian with the leader pinning matrix yields an irreducibly diagonally dominant matrix.

$H_{CC}(t_2)$ is not skew-symmetric. It then follows that $H_{\text{sym}}(t_2)w = \frac{1}{2}(H_{CC}(t_2)w + H_{CC}^\top(t_2)w) \neq 0_{N_C(t_2)}$ for all nonzero $w \in \mathbb{R}^{N_C(t_2)}$. Hence, $H_{\text{sym}}(t_2)$ has the trivial null space and 0 fails to be an eigenvalue of $H_{\text{sym}}(t_2)$. Furthermore, $H_{\text{sym}}(t_2)$ is a diagonally dominant matrix by construction with nonnegative eigenvalues by the Gershgorin disk theorem. Since $H_{\text{sym}}(t_2)$ is a symmetric matrix with positive real eigenvalues, $H_{\text{sym}}(t_2)$ is positive definite.

We next show $E_1^\top(H(t)\otimes I_n)E_1 \geq \Lambda_{\min}\|E_1\|^2$ for all $t \geq 0$, where $\Lambda_{\min} \in \mathbb{R}_{>0}$. By the Rayleigh quotient, it follows that $E_{1,C}^\top(H_{CC}(t_2)\otimes I_n)E_{1,C} \geq \lambda_{\min}(H_{\text{sym}}(t_2)\otimes I_n)E_{1,C}^\top E_{1,C}$. Since $E_{1,B}^\top E_{1,B} = 0$, $E_{1,C}^\top(H_{CC}(t_2)\otimes I_n)E_{1,C} \geq \lambda_{\min}(H_{\text{sym}}(t_2)\otimes I_n)\overline{E}_1^\top\overline{E}_1$. Since $E_1^\top(H(t_2)\otimes I_n)E_1 = E_{1,C}^\top(H_{CC}(t_2)\otimes I_n)E_{1,C}$, $E_{1,C}^\top(H_{CC}(t_2)\otimes I_n)E_{1,C} \geq \lambda_{\min}(H_{\text{sym}}(t_2)\otimes I_n)\overline{E}_1^\top\overline{E}_1$, and $\overline{E}_1^\top\overline{E}_1 = E_1^\top E_1$, $E_1^\top(H(t_2)\otimes I_n)E_1 \geq \lambda_{\min}(H_{\text{sym}}(t_2)\otimes I_n)E_1^\top E_1$. Since t_2 was arbitrary, $E_1^\top(H(t)\otimes I_n)E_1 \geq \lambda_{\min}(H_{\text{sym}}(t)\otimes I_n)\|E_1\|^2$ for all $t \geq 0$. Let $\lambda_{\min}(\mathcal{H}_{\text{sym}}) \triangleq \{\lambda_{\min}(H_{\text{sym}}(t)\otimes I_n) : t \geq 0\} \subset (0,\infty)$. Since $\lambda_{\min}(H_{\text{sym}}(t)\otimes I_n) > 0$ for all $t \geq 0$ and $\lambda_{\min}(\mathcal{H}_{\text{sym}}) \neq \varnothing$, $\lambda_{\min}(\mathcal{H}_{\text{sym}})$ is a nonempty set that is bounded below. Hence, $\Lambda_{\min} \triangleq \inf(\lambda_{\min}(\mathcal{H}_{\text{sym}})) \in \mathbb{R}_{>0}$.

C. Proof of Theorem 2

Proof: Similar argument to proof of Theorem 3.

D. Proof of Theorem 3

Proof: Let $t \geq t_k^i \geq 0$ and $i \in \mathcal{V}$. Substituting (1), (7), and (8) into the time-derivative of (3) yields $\dot{e}_{2,i}(t) \overset{a.e.}{=} -f_i(x_i(t)) - k_1 z_i(t) - k_2 e_{2,i}(t) - d_i(t)$. By Assumption 3, $\|d_i(t)\| \leq d_{i,\max}$. Recall that $x_i(t) \in \mathcal{L}_\infty$ and $z_i(t) \in \mathcal{L}_\infty$ from the proof of Theorem 1. Therefore, there exists $x_{i,\max} \in \mathbb{R}_{>0}$ and $z_{i,\max} \in \mathbb{R}_{>0}$, such that $\|x_i(t)\| \leq x_{i,\max}$ and $\|z_i(t)\| \leq z_{i,\max}$, respectively. Since $\|x_i(t)\| \leq x_{i,\max}$, Assumption 1 implies that $\|f_i(x_i(t))\| \leq f_{i,\max}$ for some $f_{i,\max} \in \mathbb{R}_{>0}$. It then follows that $\|\dot{e}_{2,i}(t)\| \leq k_2\|e_{2,i}(t)\| + \theta_{i,\max}$, where $\theta_{i,\max} \geq f_{i,\max} + k_1 z_{i,\max} + d_{i,\max} \in \mathbb{R}_{>0}$. Let $\upsilon_i : [t_k^i, \infty) \to \mathbb{R}_{\geq 0}$ satisfy $\dot{\upsilon}_i(t) = k_2\upsilon_i(t) + \theta_{i,\max}$ with initial condition $\upsilon_i(t_k^i) = \|e_{2,i}(t_k^i)\|$. Then, $\upsilon_i(t_k^i) = 0$ and

$$\upsilon_i(t) = \frac{\theta_{i,\max}}{k_2}(e^{k_2(t-t_k^i)} - 1).$$

Observe that

$$\frac{d}{dt}\|e_{2,i}(t)\| = \frac{e_{2,i}^\top(t)\dot{e}_{2,i}(t)}{\|e_{2,i}(t)\|} \overset{a.e.}{\leq} \|\dot{e}_{2,i}(t)\|.$$

Since $\frac{d}{dt}\|e_{2,i}(t)\| \overset{a.e.}{\leq} \|\dot{e}_{2,i}(t)\|$ and $\|\dot{e}_{2,i}(t)\| \leq k_2\|e_{2,i}(t)\| + \theta_{i,\max}$, it follows that $\frac{d}{dt}\|e_{2,i}(t)\| \overset{a.e.}{\leq} k_2\|e_{2,i}(t)\| + \theta_{i,\max}$. Using the solution of $\frac{d}{dt}\|e_{2,i}(t)\| \overset{a.e.}{\leq} k_2\|e_{2,i}(t)\| + \theta_{i,\max}$ and $\upsilon_i(t) = \frac{\theta_{i,\max}}{k_2}(e^{k_2(t-t_k^i)} - 1)$, we see that $\|e_{2,i}(t)\| \leq \upsilon_i(t)$ for all $t \in [t_k^i, \infty)$. Since $\|e_{2,i}(t)\| \leq \upsilon_i(t)$ and $\upsilon_i(t) = \frac{\theta_{i,\max}}{k_2}(e^{k_2(t-t_k^i)} - 1)$, equation (20) yields (31).

E. Control Algorithm

Algorithm 1: Control Algorithm for Follower i.

Select $\Lambda_{\max} > 0$ and $\Lambda_{\min} > 0$ according to Lemmas 1 and 2, respectively.
Select $x_0(0)$, $x_i(0)$, $\hat{x}_i(0)$, and υ_i for all $i \in \mathcal{V}$.
Set $N = |\mathcal{V}|$. Select $b_{\max} > 0$.
Select κ, c_0, ε, $k_{1,3}$, $k_{2,1}$, ρ_1, ρ_2, δ_1, δ_2, and $k_{1,2}$ according to (21) and $E(0) \in \mathcal{S}_\mathcal{D}$.
Compute $k_1 = \frac{1}{\Lambda_{\min}}(k_{1,1} + \frac{\rho_1^2}{\delta_1})$, $k_2 = k_{2,1} + \frac{\rho_2^2}{\delta_2}$, and $k_{1,1} = k_{1,2} + k_{1,3}$.
Compute ϕ_1 through ϕ_6 according to (17).
Set $\tau_{ij}(0) = 1$ and $\zeta_{ij}(0) = 1$ for all $i, j \in \mathcal{V}$.
Select $s_1 > 0$, $\zeta_{\min} \in [0,1]$, $t_{\text{reset}} > 0$, $\eta_\tau > 0$, and $\eta_\zeta > 0$.
Select $\vartheta > 0$, $r \in (0, R)$, and $\Delta_i > 0$ for all $i \in \mathcal{V}$.
Set $k(i) = 0$ and $t_0^i = 0$ for all $i \in \mathcal{V} \cup \{0\}$.
Set $a_{ij}(t) = 1$ for all $j \in \mathcal{N}_i(0)$.
Set $\hat{x}_j(t) = x_j(t_{k(j)}^j)$ for all $j \in \mathcal{N}_i(0) \cup \{i\}$.
if $0 \in \mathcal{N}_i(0)$ **then**
  Set $\hat{x}_0(t) = x_0(t_{k(0)}^0)$. Set $b_i(t) = b_{\max}$.
end if
while true **do**
  Compute $\zeta_{ij}(t)$ according to (5) for each $j \in \mathcal{N}_i(t)$.
  Compute $a_{ij}(t)$ according to (6) for each $j \in \mathcal{N}_i(t)$.
  Compute $z_i(t)$ according to (9).
  Compute $e_{2,i}(t) = \hat{x}_i(t) - x_i(t)$.
  Compute $u_i(t) = g_i^+(x_i(t))(k_1 z_i(t) + k_2 e_{2,i}(t))$.
  if $\phi_4\|e_{2,i}(t)\|^2 \geq \phi_5\|z_i(t)\|^2 + \frac{\varepsilon}{N}$ **then**
    Set $k(i) = k(i) + 1$. Set $t_{k(i)}^i = t$.
    Set $\hat{x}_i(t) = x_i(t_{k(i)}^i)$.
    Broadcast $x_i(t_{k(i)}^i)$ to all $j \in \mathcal{N}_i(t)$.
    Broadcast $\zeta_{ij}(t_{k(i)}^i)$ to all $j \in \mathcal{N}_i(t)$.
  end if
  if agent $j \in \mathcal{N}_i(t) \cup \{0\}$ broadcasts **then**
    Set $k(j) = k(j) + 1$. Set $t_{k(j)}^j = t$.
    Receive $x_{j,1}(t_{k(j)}^j)$. Set $\hat{x}_j(t) = x_{j,1}(t_{k(j)}^j)$.
    Measure $x_{j,2}(t_{k(j)}^j)$.
    Receive $\zeta_{jp}(t_{k(j)}^j)$ for each $p \in \mathcal{N}_j(t)$.
    if $\omega_{ij}(t_{k(j)}^j) \leq r$ and $\Delta t_{k(j)}^j \leq \Delta_j$ **then**
      Compute $\Psi_{ij}(t_{k(j)}^j)$ according to (4) for each $t_{k(j)}^j \in S_j$.
    else
      Set $\Psi_{ij}(t_{k(j)}^j) = \vartheta$.
    end if
    Set $S_j = \{t_{k(j)}^j : t - t_{\text{reset}} \leq t_{k(j)}^j < t\}$.
    Store $\{\Psi_{ij}(t_{k(j)}^j) : t_{k(j)}^j \in S_j\}$.
    Compute $\tau_{ij}(t) = \frac{1}{|S_j|}\sum_{t_{k(j)}^j \in S_j} e^{-s_1\Psi_{ij}(t_{k(j)}^j)}$.
  end if
end while

References

[1] A. Adaldo *et al.*, "Event-triggered pinning control of switching networks," *IEEE Trans. Control Netw. Syst.*, vol. 2, no. 2, pp. 204–213, Jun. 2015.

[2] D. V. Dimarogonas, E. Frazzoli, and K. H. Johansson, "Distributed event-triggered control for multi-agent systems," *IEEE Trans. Autom. Control*, vol. 57, no. 5, pp. 1291–1297, May 2012.

[3] T. H. Cheng, Z. Kan, J. R. Klotz, J. M. Shea, and W. E. Dixon, "Event-triggered control of multi-agent systems for fixed and time-varying network topologies," *IEEE Trans. Autom. Control*, vol. 62, no. 10, pp. 5365–5371, Oct. 2017.

[4] X. Dong and G. Hu, "Time-varying formation control for general linear multi-agent systems with switching directed topologies," *Automatica*, vol. 73, pp. 47–55, 2016.

[5] C. Nowzari and J. Cortés, "Distributed event-triggered coordination for average consensus on weight-balanced digraphs," *Automatica*, vol. 68, pp. 237–244, 2016.

[6] P. Tabuada, "Event-triggered real-time scheduling of stabilizing control tasks," *IEEE Trans. Autom. Control*, vol. 52, no. 9, pp. 1680–1685, Sep. 2007.

[7] W. Heemels, K. Johansson, and P. Tabuada, "An introduction to event-triggered and self-triggered control," in *Proc. IEEE Conf. Decis. Control*, Dec. 2012, pp. 3270–3285.

[8] E. Garcia, Y. Cao, and D. W. Casbeer, "Decentralized event-triggered consensus with general linear dynamics," *Automatica*, vol. 50, no. 10, pp. 2633–2640, 2014.

[9] Y. Fan, L. Liu, G. Feng, and Y. Wang, "Self-triggered consensus for multi-agent systems with zeno-free triggers," *IEEE Trans. Autom. Control*, vol. 60, no. 10, pp. 2779–2784, Oct. 2015.

[10] Z. Feng and G. Hu, "Secure cooperative event-triggered control of linear multi-agent systems under DoS attacks," *IEEE Trans. Control Syst. Tech.*, vol. 28, no. 3, pp. 741–752, May 2020.

[11] A. Sargolzaei, K. K. Yen, and M. N. Abdelghani, "Preventing time-delay switch attack on load frequency control in distributed power systems," *IEEE Trans. Smart Grid*, vol. 7, no. 2, pp. 1176–1185, Mar. 2015.

[12] N. H. Vaidya, L. Tseng, and G. Liang, "Iterative approximate byzantine consensus in arbitrary directed graphs," in *Proc. ACM Symp. Prin. Distrib. Comput.*, 2012, pp. 365–374.

[13] F. M. Zegers, P. Deptula, J. M. Shea, and W. E. Dixon, "Event-triggered approximate leader-follower consensus with resilience to byzantine adversaries," in *Proc. IEEE Conf. Decis. Control*, Nice, France, Dec. 2019, pp. 6412–6417.

[14] H. J. LeBlanc, H. Zhang, X. Koutsoukos, and S. Sundaram, "Resilient asymptotic consensus in robust networks," *IEEE J. Sel. Areas Commun.*, vol. 31, no. 4, pp. 766–781, Apr. 2013.

[15] J. Usevitch and D. Panagou, "Resilient leader-follower consensus to arbitrary reference values," in *Proc. Annu. Amer. Control Conf.*, 2018, pp. 1292–1298.

[16] S. M. Dibaji and H. Ishii, "Resilient consensus of second-order agent networks: Asynchronous update rules with delays," *Automatica*, vol. 81, pp. 123–132, 2017.

[17] J. R. Klotz, A. Parikh, T.-H. Cheng, and W. E. Dixon, "Decentralized synchronization of uncertain nonlinear systems with a reputation algorithm," *IEEE Trans. Control Netw. Syst.*, vol. 5, no. 1, pp. 434–445, Mar. 2018.

[18] L. Consolini, F. Morbidi, D. Prattichizzo, and M. Tosques, "Leader-follower formation control of nonholonomic mobile robots with input constraints," *Automatica*, vol. 44, pp. 1343–349, 2008.

[19] F. Zegers, M. Hale, J. M. Shea, and W. E. Dixon, "Reputation-based event-triggered formation control and leader tracking with resilience to byzantine adversaries," in *Proc. Annu. Amer. Control Conf.*, 2020, pp. 761–766.

[20] A. V. Proskurnikov, A. S. Matveev, and M. Cao, "Opinion dynamics in social networks with hostile camps: Consensus vs. polarization," *IEEE Trans. Autom. Control*, vol. 61, no. 6, pp. 1524–1536, Jun. 2015.

[21] W. Xia, M. Cao, and K. H. Johansson, "Structural balance and opinion separation in trust-mistrust social networks," *IEEE Trans. Control Netw. Syst.*, vol. 3, no. 1, pp. 46–56, Mar. 2016.

[22] Z. Cai, M. S. de Queiroz, and D. M. Dawson, "A sufficiently smooth projection operator," *IEEE Trans. Autom. Control*, vol. 51, volume. 1, pp. 135–139, Jan. 2006.

[23] R. Kamalapurkar, J. A. Rosenfeld, J. Klotz, R. J. Downey, and W. E. Dixon, "Supporting lemmas for rise-based control methods," 2014, *arXiv:1306.3432.*

[24] B. E. Paden and S. S. Sastry, "A calculus for computing Filippov's differential inclusion with application to the variable structure control of robot manipulators," *IEEE Trans. Circuits Syst.*, vol. 34, no. 1, pp. 73–82, Jan. 1987.

[25] D. Shevitz and B. Paden, "Lyapunov stability theory of nonsmooth systems," *IEEE Trans. Autom. Control*, vol. 39 no. 9, pp. 1910–1914, Sep. 1994.

[26] R. A. Horn and C. R. Johnson, *Matrix Analysis.* Cambridge, U.K.: Cambridge Univ. Press, 1990.

[27] M. Mesbahi and M. Egerstedt, *Graph Theoretic Methods in multi-agent Networks*. Princeton, NJ, USA: Princeton Univ. Press, 2010.

Federico M. Zegers received the B.S. degree in mechanical engineering and the B.S. degree in mathematics, and the M.S. degree in mechanical engineering from the University of Florida, Gainesville, FL, USA, in 2016, and 2019, respectively. He is currently working towards the Ph.D. degree in mechanical engineering under the supervision of Dr. Warren Dixon at the University of Florida.

His research interests include Lyapunov-based nonlinear and adaptive control, multi-agent systems, switched/hybrid systems theory, and robotics.

Matthew T. Hale (Member, IEEE) received the B.S.E. degree in electrical engineering summa cum laude from the University of Pennsylvania, Philadelphia, PA, USA, in 2012, and the M.S. and Ph.D. degrees in electrical and computer engineering from the Georgia Institute of Technology, in Atlanta, GA, USA, 2015 and 2017, respectively.

He is an Assistant Professor of Mechanical and Aerospace Engineering with the University of Florida, Gainesville, FL, USA. He directs the Control, Optimization, and Robotics Engineering (CORE) Lab, at the University of Florida. His research interests include multi-agent systems, mobile robotics, privacy in control, distributed optimization, and graph theory.

Dr. Hale was the recipient of the Teacher of the Year award in the UF Department of Mechanical and Aerospace Engineering for the 2018–2019 school year, and the recipient of the NSF CAREER Award in 2020 for his work on privacy in control systems.

John M. Shea (Member, IEEE) received the B.S. degree in computer engineering, and the M.S. and Ph.D. degrees in electrical engineering from Clemson University, Clemson, SC, USA, in 1993, 1995 and 1998, respectively.

In 1999, he joined as the faculty with the Department of Electrical and Computer Engineering, at the University of Florida, Gainesville, FL, USA, where he was promoted to the rank of Professor, in 2015. His research interests include wireless and military communications and networked autonomous systems.

Dr. Shea was the recipient of the Technical Achievement Award for contributions to military communications from the IEEE Military Communications Conference (MILCOM), in 2012, the Ellersick Award from the IEEE Communications Society for the Best Paper in the Unclassified Program of MILCOM, in 1996 and 2013, and the Outstanding Young Alumni award from the Clemson University College of Engineering and Science, in 2011. He was selected as a Finalist for the 2004 Eta Kappa Nu Outstanding Young Electrical Engineer. He has been an Editor for IEEE WIRELESS COMMUNICATIONS magazine, since 2010. He was an Editor for the IEEE TRANSACTIONS ON WIRELESS COMMUNICATIONS, from 2008 to 2012, and was an Associate Editor for the IEEE TRANSACTIONS ON VEHICULAR TECHNOLOGY, from 2002 to 2007. He was the Technical Program Chair for the Unclassified Program of MILCOM, in 2010.

Warren E. Dixon (Fellow, IEEE) received the Ph.D. degree in electrical engineering from the Department of Electrical and Computer Engineering from Clemson University, Clemson, SC, USA, in 2000.

He was selected as a Eugene P. Wigner Fellow and worked as a staff Researcher at Oak Ridge National Laboratory. In 2004, he joined the Mechanical and Aerospace Engineering Department, the University of Florida, Gainesville, FL, USA, where he currently is the Newton C. Ebaugh Professor and Department Chair. His research interests include the development and application of Lyapunov-based control techniques for uncertain nonlinear systems.

Dr. Dixon is an ASME and IEEE Fellow for contributions to adaptive control of uncertain nonlinear systems. He was the recipient of various career and best paper awards.